

Article

Discovery of Oral VEGFR-2 Inhibitors with Prolonged Ocular Retention that are Efficacious in Models of Wet Age-Related Macular Degeneration

Erik L Meredith, Nello Mainolfi, Stephen Poor, Yubin Qiu, Karl Miranda, James Powers, Donglei Liu, Fupeng Ma, Catherine Solovay, Chang Rao, Leland Johnson, NAN JI, Gerald Artman, Leo Hardegger, Shawn Hanks, Siyuan Shen, Amber Woolfenden, Elizabeth Fassbender, Jeremy Sivak, Yiqin Zhang, Debby Long, Rosemarie Cepeda, Fang Liu, Vinayak P. Hosagrahara, Wendy Lee, Peter Tarsa, Karen Anderson, Jason Elliott, and Bruce Jaffee

J. Med. Chem., **Just Accepted Manuscript** • DOI: 10.1021/acs.jmedchem.5b01227 • Publication Date (Web): 15 Nov 2015

Downloaded from <http://pubs.acs.org> on November 16, 2015

Just Accepted

“Just Accepted” manuscripts have been peer-reviewed and accepted for publication. They are posted online prior to technical editing, formatting for publication and author proofing. The American Chemical Society provides “Just Accepted” as a free service to the research community to expedite the dissemination of scientific material as soon as possible after acceptance. “Just Accepted” manuscripts appear in full in PDF format accompanied by an HTML abstract. “Just Accepted” manuscripts have been fully peer reviewed, but should not be considered the official version of record. They are accessible to all readers and citable by the Digital Object Identifier (DOI®). “Just Accepted” is an optional service offered to authors. Therefore, the “Just Accepted” Web site may not include all articles that will be published in the journal. After a manuscript is technically edited and formatted, it will be removed from the “Just Accepted” Web site and published as an ASAP article. Note that technical editing may introduce minor changes to the manuscript text and/or graphics which could affect content, and all legal disclaimers and ethical guidelines that apply to the journal pertain. ACS cannot be held responsible for errors or consequences arising from the use of information contained in these “Just Accepted” manuscripts.

SCHOLARONE™
Manuscripts

1
2
3
4
5
6
7
8
9
10
11
12
13
14
15
16
17
18
19
20
21
22
23
24
25
26
27
28
29
30
31
32
33
34
35
36
37
38
39
40
41
42
43
44
45
46
47
48
49
50
51
52
53
54
55
56
57
58
59
60

1
2
3
4
5
6
7
8
9
10
11
12
13
14
15
16
17
18
19
20
21
22
23
24
25
26
27
28
29
30
31
32
33
34
35
36
37
38
39
40
41
42
43
44
45
46
47
48
49
50
51
52
53
54
55
56
57
58
59
60

Discovery of Oral VEGFR-2 Inhibitors with Prolonged Ocular Retention that are Efficacious in Models of Wet Age-Related Macular Degeneration

Erik L. Meredith^{a}, Nello Mainolfi^{a†}, Stephen Poor^b, Yubin Qiu^b, Karl Miranda^{a1}, James Powers^a, Donglei Liu^a, Fupeng Ma^a, Catherine Solovay^a, Chang Rao^{a#}, Leland Johnson^{a‡}, Nan Ji^{aϕ}, Gerald Artman^{a1}, Leo Hardegger^{aζ}, Shawn Hanks^b, Siyuan Shen^b, Amber Woolfenden^b, Elizabeth Fassbender^b, Jeremy Sivak^{b‡}, Yiqin Zhang^{b‡}, Debby Long^b, Rosemarie Cepeda^b, Fang Liu^b, Vinayak P. Hosagrahara^{cb}, Wendy Lee^c, Peter Tarsa^d, Karen Anderson^b, Jason Elliott^a, Bruce Jaffee^b*

^aNovartis Institutes for BioMedical Research, Global Discovery Chemistry, 100 Technology Square, Cambridge, MA 02139

^bNovartis Institutes for BioMedical Research, Ophthalmology, 500 Technology Square, Cambridge, MA 02139

^cNovartis Institutes for BioMedical Research, Metabolism and Pharmacokinetics, 250 Massachusetts Avenue, Cambridge MA, 02139

^dNovartis Institutes for BioMedical Research, Chemical and Pharmaceutical Profiling, 500 Technology Square, Cambridge, MA 02139

erik.meredith@novartis.com

KEYWORDS. vascular endothelial growth factor, VEGF, VEGF-R, receptor tyrosine kinase, KDR, kinase inhibitor, age-related macular degeneration, angiogenesis, choroidal neovascularization.

ABSTRACT

The benefit of intravitreal anti-VEGF therapy in treating wet age-related macular degeneration (AMD) is well established. Identification of VEGFR-2 inhibitors with optimal ADME properties for an ocular indication provides opportunities for dosing routes beyond intravitreal injection. To identify such inhibitors, we employed a high-throughput *in vivo* screening strategy with rodent models of choroidal neovascularization and iterative compound design to identify VEGFR-2 inhibitors with potential to benefit wet AMD patients. These compounds demonstrate preferential ocular tissue distribution and efficacy after oral administration while minimizing systemic exposure.

Introduction

Age-related macular degeneration (AMD) is an eye disease that causes vision loss due to pathology in the macula, the area of the retina that enables sharp and detailed vision. AMD is responsible for the majority of cases of blindness and visual impairment in aged adults. In the wet form of AMD, choroidal blood vessels (choroidal neovascularization, CNV) sprout and expand into the sub-macular space leaking fluid and blood. This leads to retinal edema, scar tissue formation and irreversible damage to the macula. The current approved therapies for wet AMD are the anti-VEGF-A antibody ranibizumab, the anti-VEGF-A aptamer pegaptanib, and

1
2
3 the anti-VEGF-A and PLGF fusion protein aflibercept. All are delivered by intravitreal
4 injection (IVT), a procedure that carries a small, but significant, risk of blinding complications
5 including endophthalmitis, retinal detachment or uveitis. Ranibizumab and aflibercept are the
6 most effective, stabilizing vision in 60% patients and significantly improving vision (gain of 3
7 lines of vision on an ETDRS reading chart) in approximately 1/3 of patients.¹ Injections are
8 administered monthly or bi-monthly, which is a significant burden for patients and retinal
9 doctors. Even with anti-VEGF therapy, wet AMD patients still have substantial visual deficit.²
10 We envisioned an opportunity for a less invasive wet AMD therapy based on an orally available
11 inhibitor of the receptor tyrosine kinase (RTK) VEGFR-2 (KDR, Flt-1). An oral therapy may
12 provide greater efficacy than intravitreal therapy by enabling more frequent dosing and greater
13 target tissue exposure.
14
15
16
17
18
19
20
21
22
23
24
25
26
27
28

29 The role of VEGF-A in the regulation of angiogenesis is well established. Although new
30 vessel growth and maturation are highly complex processes, requiring the sequential activation
31 of a series of receptors by numerous ligands, VEGF-A signaling is a critical rate-limiting step.³
32 VEGF-A promotes growth of vascular endothelial cells and is also known to induce vascular
33 leakage.⁴ Ocular VEGF-A levels are increased in preclinical models and human diseases of
34 ocular angiogenesis including wet AMD^{5,6}, diabetic retinopathy and retinal vein occlusions^{7,8}.
35
36
37
38
39
40
41
42

43 VEGF-A binds to two related receptor tyrosine kinases, VEGFR-1 and VEGFR-2, which both
44 have an extracellular domain consisting of 7 immunoglobulin-like domains, a single
45 transmembrane region, and a consensus tyrosine kinase sequence that is interrupted by a kinase-
46 insert domain.⁹ VEGFR-2 (KDR or Flt-1) is implicated in all aspects of normal and pathological
47 vascular endothelial cell biology. VEGFR-2 is the major mediator of the mitogenic, angiogenic,
48 and permeability-enhancing effects of VEGF-A. VEGFR-2 null mice die *in utero* between days
49
50
51
52
53
54
55
56
57
58
59
60

1
2
3 8.5-9.5 and are characterized by a lack of vasculogenesis and failure to develop organized blood
4 vessels.¹⁰ Upon VEGF-A binding, VEGFR-2 undergoes dimerization and ligand-dependent
5
6 tyrosine phosphorylation in intact cells, resulting in a mitogenic, chemotactic and survival
7
8 signal.¹¹
9
10

11
12 Systemic inhibition of VEGF pathway is known to cause on-target side effects including
13 hypertension, proteinuria, bleeding, thromboembolism, and gastrointestinal perforation.¹² Our
14
15 strategy to mitigate the risk of systemic VEGF inhibition was to identify compounds with
16
17 preferential distribution and retention in ocular tissues (retina and retinal pigment
18
19 epithelium/choroid) compared to the plasma.
20
21

22
23
24 There are a number of approved orally administered VEGFR-2 inhibitors for oncology
25
26 indications and several have been investigated in wet AMD.¹³⁻¹⁵ In a published case study,
27
28 treatment with oral sorafenib correlated with reduced retinal edema and increased visual
29
30 acuity.^{16,17} More recently, orally dosed pazopanib is reported to improve vision, reduce edema,
31
32 and reduce neovascularization in wet AMD patients.¹⁸ Despite the fact the doses used were
33
34 markedly less than those in oncology indications, systemic side effects were still observed.
35
36 Thus, a compound that more selectively targets ocular tissues than marketed oncology drugs
37
38 would potentially be an effective and safe therapy for wet AMD patients.
39
40
41

42
43 To achieve our objective of identifying compounds with preferential ocular distribution we
44
45 understood that relatively high-throughput *in vivo* models of ocular angiogenesis would be
46
47 needed to establish both ocular efficacy and tissue distribution relationships. The primary *in vivo*
48
49 models utilized were laser-induced choroidal neovascularization (CNV) in mice and in rats.
50
51 Briefly, photocoagulating green laser pulses are applied to the eye in order to cause a focal
52
53 rupture of Bruch's membrane, an extracellular matrix between the retina and choroid. Rupture
54
55
56
57
58
59
60

1
2
3 of Bruch's membrane induces production of local inflammatory factors and VEGF resulting in
4 choroidal neovascularization (CNV). CNV formation in response to laser injury has been
5 demonstrated in humans, monkeys, pigs, and rodents and is a VEGF-dependent pathology.¹⁹
6
7

8
9
10 Evaluation of several internal VEGFR-2 kinase inhibitors in the mouse CNV model provided
11 **1**²⁰ (Table 1) as a promising starting point for chemistry optimization. The compound
12 demonstrated a modest level of inhibition (44%), but had poor aqueous solubility (<5 μ M at pH
13 6.8). Thus, we undertook a strategy to identify compounds with greater efficacy and improved
14 ADME properties.
15
16
17
18
19
20
21
22
23

24 Chemistry

25
26
27 The preparation of monocyclic pyrimidine analogs such as **6** was carried out as described
28 in Scheme 1. Coupling of indole **2** with pyrimidine **3**²¹ was achieved by treatment with DBU.
29 Formation of the urea was then accomplished by trapping the lithium anion of the indole with the
30 desired phenylisocyanates. Removal of the benzyl protecting group with TFA provided alcohol
31 **5**, which was readily converted to methylamine **6** by conversion first to the mesylate and then
32 displacement with methylamine.
33
34
35
36
37
38
39
40

41 The bicyclic pyrimidine intermediates **8** and **10** were accessible from the corresponding β -
42 ketoesters **7** and **9** respectively (Scheme 2). Treatment of each β -ketoester **7** and **9** with
43 formamidine acetate provided the corresponding hydroxypyrimidine, which then underwent a
44 protecting group swap from benzyl to Boc. Conversion to the chloropyrimines **8** and **10** was
45 then accomplished by reaction with carbon tetrachloride and triphenylphosphine.
46
47
48
49
50
51
52
53
54
55
56
57
58
59
60

1
2
3 The 8-methyl substituted bicyclic pyrimidine **15** was prepared as outlined in Scheme 3. The β -
4 ketoester **14** was converted to the corresponding Boc protected chloropyrimidine by analogy to
5 that of **8** and **10**.
6
7

8
9
10 The chiral chloropyrimidines **21** and **22** were prepared starting from (*S*)- α -
11 methylbenzylamine, which underwent reductive amination with **16** and then ethyl glyoxylate to
12 provide diester **18** (Scheme 4). Claisen condensation of **18** then provided diastereomers **19** and
13 **20**, which were separated by flash chromatography. Conversion of each diastereomer **19** and **20**
14 to the corresponding chloropyrimidines **21** and **22** was achieved under the same conditions as
15 described above.
16
17
18
19
20
21
22
23

24 The 6,5-bicyclic pyrimidine **24** was prepared by condensation of the commercially available β -
25 ketoester **23** with formamidine acetate (Scheme 5). Construction of the methyl substituted 6,5-
26 bicyclic pyrimidine was as described in Scheme 6. In each of these cases the hydroxy
27 pyrimidines were used in the subsequent coupling steps as the chloro derivatives were found to
28 be both difficult to prepare and use due to instability.
29
30
31
32
33
34
35

36 Coupling of the bicyclic pyrimidines **10**, **15**, **21**, and **22** to the hydroxyindole was achieved by
37 treatment with DBU to give the corresponding derivatives **30** (Scheme 7). The 6,5-bicyclic
38 pyrimidines **24** and **28** were efficiently coupled to **29** with PyBop and DBU.²² Formation of the
39 desired urea analogs **33** was achieved by treatment of the sodium anion of **30** with either a
40 preformed phenylcarbamate or a commercially available isocyanate. The aminopyrazoles and
41 aminoisoxazoles **31** that were not commercially available were prepared as described
42 previously.^{23, 24} The Boc protecting group was then removed upon treatment with TFA to
43 provide the desired compounds **33** for testing against VEGFR-2.
44
45
46
47
48
49
50
51
52
53
54
55
56
57
58
59
60

Compound evaluation

In vitro inhibition of VEGFR-2 receptor tyrosine kinase was assessed with two primary assays; a KDR receptor tyrosine kinase biochemical assay and a cellular assay with BaF3-Tel-KDR cells that are engineered to constitutively require VEGFR-2 kinase domain activity for survival and proliferation. Select compounds were evaluated for selectivity in a panel of 62 kinases.

Early in our effort it was found that some of the compounds also inhibited hERG, which is a potassium ion channel that can cause long QT syndrome and cardiac dysfunction. As we aimed to minimize the systemic risk associated, compounds were analyzed in an automated Q-patch assay to determine their activity on the hERG channel.²⁵

As we sought to identify compounds that selectively distributed to the ocular tissues, we did not apply usual *in vitro* PK-ADME filters prior to *in vivo* evaluation. Priority was given to compounds that had demonstrated good aqueous solubility²⁶, yet generally those with good *in vitro* potency were selected for evaluation in the mouse laser CNV model (C57BL/6) at a single dose of 10 mg/kg (*p.o.*). This screening dose was selected based on early efficacy studies with existing VEGFR-2 inhibitors, such as **1**, and was not expected to cause any acute side effects that would compromise a given study. Compounds were formulated as suspensions (0.5% methyl cellulose, Tween[®] 80, and water) to better inform our understanding of their intrinsic ADME properties. Each compound was dosed starting the day of laser application and continued daily with the last dose given on day 6 and CNV area measurement on day 7. Comparison of CNV area in animals dosed with compound or placebo was used to establish percent inhibition.

Compounds exhibiting >60 % inhibition at the 10 mg/kg screening dose were further evaluated in mouse CNV dose response studies to establish ED₅₀ and ED₉₀ relationships. Compounds with an ED₉₀ < 20 mg/kg in the mouse CNV assay were then characterized in the rat laser CNV model

1
2
3 (Brown Norway). To understand the correlation between efficacy and exposure, the distribution
4 profiles for select compounds were determined by orally dosing Brown Norway rats and
5
6 measuring time course drug exposures in the plasma and ocular tissues (retina and retinal
7
8 pigment epithelium/choroid/sclera complex). Further understanding of the ADME profiles for
9
10 select compounds was accomplished by discrete *i.v./p.o.* PK studies in Brown Norway rats.
11
12
13
14
15
16
17

18 **Results**

19
20 Early on we recognized the need to improve on the aqueous solubility of compound **1**. It was
21 anticipated that greater aqueous solubility would provide increased oral bioavailability and as a
22 consequence better efficacy. X-ray co-crystal structures of related VEGFR-2 inhibitors indicated
23 that incorporation of ionizable groups on the pyrimidine should be possible. An important early
24 finding was that the aminopyrimidine of **1** was not required for potency as **5a** proved to be
25 equipotent in the biochemical assay and have similar efficacy in the mouse CNV model (Table 1;
26 45% inhibition). A basic amine was introduced to give compound **6a**, which demonstrated
27 similar potency *in vitro* and importantly increased efficacy *in vivo* (67% inhibition). As
28 anticipated **6a** had improved aqueous solubility (Table 2; 64 μ M) relative to **1**. Incorporation of
29 a fluoro substituent in the 4-position of the aniline as in **6b** provided a boost in efficacy as the
30 compound showed 92% inhibition of neovascularization in the mouse at the 10 mg/kg dose.
31
32
33
34
35
36
37
38
39
40
41
42
43
44
45

46 Collectively, these compounds demonstrated the potential for optimization through inclusion
47 of the basic amine moiety, however **6b** was found to have an undesirable level of activity on the
48 hERG channel (table 3; IC₅₀ 5800 nM). To optimize *in vivo* efficacy while balancing hERG
49 activity and aqueous solubility we focused our efforts on the basic amine region and the urea side
50 chain of **6b**. Our exploration centered on altering both the pKa and the steric environment of the
51
52
53
54
55
56
57
58
59
60

1
2
3 amine as well as reducing the lipophilicity of the urea side chain. It was thought that a
4
5 combination of these changes would provide the desired efficacy while reducing the hERG
6
7 liability.
8
9

10 Rigidification of the amine side chain by incorporation into the 6,6-bicyclic pyrimidine **33a**
11
12 was well tolerated as it gave 87% inhibition in the mouse CNV model with modest aqueous
13
14 solubility (84 μM). However, no substantial reduction in hERG activity was realized (IC_{50} 8900
15
16 nM). Intriguingly, the isomeric 6,6-bicyclic pyrimidine **33b** provided no significant inhibition *in*
17
18 *vivo* despite having good potency in the enzymatic and cellular assays.
19
20

21 To further probe the sensitivity of this region to substitution, the enantiomeric methyl analogs
22
23 **33c** and **33d** were prepared. These compounds again highlighted a similar pattern of disconnect
24
25 between the *in vitro* and the *in vivo* efficacy as **33c**, the (*S*)-enantiomer, demonstrated greater
26
27 efficacy despite similar *in vitro* potency to the (*R*)-enantiomer **33d**. Acetylation of the amine as
28
29 in **33e** caused a complete loss of efficacy in the mouse model, while retention of the basic amine
30
31 as in the ethyl derivative **33f** provided 81% inhibition. However, the tertiary amine **33f** reduced
32
33 the aqueous solubility (< 5 μM).
34
35
36
37

38 Reduction of amine pKa was achieved with the 6,5-bicyclic pyrimidine **33g**. This compound
39
40 was found to be efficacious (68% inhibition) in the mouse model and demonstrated reduced
41
42 hERG activity (IC_{50} 15600 nM). In this instance however, the addition of a methyl group to the
43
44 bicycle as in **33h** and **33i** attenuated the efficacy.
45
46
47

48 The pyridyl analog **33j** was designed to reduce the lipophilicity of the aniline moiety.
49
50 Although the *in vitro* potency in both the biochemical (280 nM) and cell (1922 nM) assays was
51
52 attenuated it demonstrated the potential benefit through further optimization to identify more
53
54 preferred heteroaryl groups as there was a favorable impact on aqueous solubility (190 μM).
55
56
57
58
59
60

1
2
3 Indeed, further design of heteroaryl replacements lead to pyrazoles **33k** and **33l** that provided
4 very good *in vitro* potency (cell IC₅₀ 3 nM & 1 nM respectively). While the initial pyrazole
5 analogs **33k** and **33l** provided no inhibition in the mouse CNV model, they did have markedly
6 improved aqueous solubility (833 and 682 μM respectively). Further design and optimization
7 led to the discovery that the cyclopropylmethyl analog **33m** provided 64% inhibition. The close
8 structural similarities among these analogs again provide a dramatic demonstration of the subtle
9 effects realized only with *in vivo* SAR. Pyrazole **33m**, had good aqueous solubility (252 μM)
10 and minimal hERG activity with an IC₅₀ > 30,000 nM. This was an important finding as it
11 demonstrated the ability to reduce hERG activity without alteration of the amine basicity.
12
13
14
15
16
17
18
19
20
21
22
23

24 Combining the methyl substituted 6,6-bicyclic pyrimidine with the cyclopropylmethyl
25 pyrazole as in **33n** gave good potency in the cellular assay (0.9 nM), efficacy in the mouse (67%
26 inhibition), good aqueous solubility (450 μM), and minimal hERG activity (IC₅₀ 27,400 nM). In
27 this case, as shown above, the opposite enantiomer **33p** and the 6,5-bicyclic analog **33o** showed
28 reduced efficacy *in vivo* despite similar potency *in vivo*.
29
30
31
32
33
34
35

36 Further exploration of aniline replacements revealed that the isoxazole (*e.g.* **33q** and **33r** with
37 83% and 96% inhibition respectively) provided even greater efficacy than the corresponding
38 pyrazole analogs, however they also had greater hERG activity. It was also found that the 3-
39 aminoisoxazole analogs (*e.g.* **33s**) were more active *in vivo* than the isomeric 5-aminoisoxazoles
40 (*e.g.* **33t**). Similar to the pyrazole analogs, inclusion of the methyl group in the 6,5-pyrimidine
41 did not give a favorable increase in activity (**33u**), which was again in contrast to the 6,6-bicyclic
42 pyrimidines. Modification of the isoxazole substitution from *t*-butyl to cyclopropyl **33v** or **33w**
43 provided maximal inhibition in the mouse model (98 and 96% inhibition respectively).
44
45
46
47
48
49
50
51
52
53
54
55
56
57
58
59
60

1
2
3 Isoxazole **33v** also showed minimal hERG activity with an $IC_{50} > 30,000$ nM in combination
4
5 with good aqueous solubility (110 μ M).
6
7

8 Dose response studies in the mouse and rat were conducted for the preferred compounds
9
10 identified from the mouse *in vivo* single dose screen (Table 4). In the mouse laser CNV model,
11
12 the isoxazole derivative **33v** provided the greatest efficacy on a per dose basis with an ED_{90} of
13
14 4.8 mg/kg, while its corresponding aniline analog **33g** provided an ED_{90} of 31 mg/kg. In contrast
15
16 the pyrazole analog **33n** was found to have a higher ED_{90} (19.6 mg/kg) than its corresponding
17
18 aniline derivative **33c** in the mouse CNV. Both the non-methylated **33m** and the methylated
19
20 **33n**, provided a similar dose response in the mouse model. Further characterization of **33n**, **33v**,
21
22 and **33m** in the rat laser CNV model again demonstrated that on a per dose basis **33v** was more
23
24 efficacious than either **33m** or **33n**.
25
26
27
28

29 As stated above our key objective was to identify VEGFR-2 inhibitors that provided good
30
31 efficacy in the mouse and rat laser CNV models following oral dosing, and demonstrated
32
33 distribution to and retention in the ocular tissues relative to the plasma. Discrete oral PK studies
34
35 in Brown Norway rats were conducted with preferred compounds. Exposure in plasma, retina
36
37 and posterior eye cup (retinal pigment epithelium/choroid sclera complex = posterior eye cup)
38
39 were assessed at 7 time points after dosing between 0-24 hrs. In Table 4, the dose normalized
40
41 (DN) exposures for 3 compounds are detailed. It can readily be seen that **33v** has significantly
42
43 higher plasma exposure (DNC_{max} and $DNAUC$) than either **33n** or **33m**. In the retina, **33n** and
44
45 **33v** had similar exposure while **33m** was measurably lower. In the PEC, there was even greater
46
47 contrast among the three compounds with the exposure decreasing in order from **33v** > **33n** >
48
49 **33m**. The data from the ocular tissues indicate a strong preference for retention of each of the
50
51 compounds in those tissues versus retention in the plasma. This is most easily noted by
52
53
54
55
56
57
58
59
60

1
2
3 comparison of the plasma/retina/PEC dose normalized concentrations at 24 h (**33n** 1.6/122/1067
4 nM; **33v** 6/65/3334 nM; **33m** 0.7/13/102 nM). The above data demonstrate that it is possible to
5
6 identify compounds with preferential distribution to the ocular tissues and reduced plasma
7
8 exposure. The advantage of such distribution in mitigating systemic side effects will only be
9
10 borne out in toxicology studies as it was not expected that our efficacy models would address
11
12 this. However, it is worth noting that the approved VEGFR-2 inhibitor pazopanib, described
13
14 above, has been reported to provide 93% inhibition of laser induced CNV in the mouse model
15
16 when dosed at orally at 100 mg/kg twice daily and that dose when given for 7 d produced a
17
18 plasma exposure of ~13 μM at 16 h post the last dose.²⁷
19
20
21
22
23

24 The *i.v./p.o.* PK parameters of **33n**, **33v**, and **33m** provide further detail regarding systemic
25 exposure and clearance (Table 6). In accord with the ocular PK study above, **33m** shows a
26
27 higher rate of clearance from the plasma (165 mL/min/kg) while **33v** provided much lower
28
29 clearance (6 mL/min/kg). All three of these compounds were found to have good plasma
30
31 exposure following oral dosing ($F\% > 50$). The plasma and ocular PK data highlight the
32
33 limitation of optimizing compounds with limited *in vivo* efficacy measurements or an over
34
35 reliance on *in vivo* PK as **33m** would not have been preferred either from plasma or ocular PK,
36
37 yet the compound is efficacious at reducing laser induced CNV.
38
39
40
41
42

43 In a selectivity panel consisting of 62 kinases, **33n** and **33v**, were found to have activity < 1
44
45 μM against several related kinases [IC_{50} (μM) **33n**: Ret 0.066, PDGFR α 0.15, c-Kit 0.6; **33v**:
46
47 Ret 0.50, PDGFR α 0.15 μM]. This is consistent with the observed *in vivo* efficacy being
48
49 primarily driven by VEGFR-2 inhibition.
50
51
52
53
54

55 Conclusions

56
57
58
59
60

1
2
3 Predicting ocular efficacy based on *in vitro* potency and *in vivo* exposure remains a challenge
4 in ocular drug discovery. This is in part evidenced by the high number of potent VEGFR-2
5 inhibitors described herein, which provide little or no efficacy in the mouse laser CNV model.
6
7 The challenge is more clearly illustrated by molecules **33m**, **33n**, and **33v**, which provide similar
8 *in vivo* efficacy despite substantially different tissue distribution profiles. The reason for these
9 disconnects are not fully understood at this time. We believe melanin binding plays a key role
10 not only in the preferential distribution of the compound to the ocular tissue, but also in the
11 differing correlations between ocular exposure and efficacy in the CNV models. In part the
12 answer may come from melanin binding studies that adequately provide the kinetic binding
13 profiles of the molecules. Differential kinase selectivity may provide another hypothesis to
14 explain the exposure-efficacy disconnect, although data collected against a kinase panel indicate
15 that the molecules are reasonably selective for VEGFR-2 and have similar broad profiles.
16
17
18
19
20
21
22
23
24
25
26
27
28
29
30
31

32 Despite the inability to *a priori* predict ocular efficacy based on plasma PK and potency, our
33 use of relatively high-throughput *in vivo* screening in a mouse laser CNV model facilitated the
34 generation of clear and actionable *in vivo* SAR. Through optimization of one particular series of
35 VEGFR-2 inhibitors, described herein, multiple promising compounds were identified that
36 effectively reduced choroidal neovascularization and provide preferential distribution to the
37 ocular tissues. The observations made with **33m**, **33n**, and **33v** are a clear demonstration of the
38 ability to identify VEGFR-2 inhibitors with markedly higher ocular exposure than in the plasma.
39
40
41
42
43
44
45
46
47

48 Selective distribution to the target tissue of interest, the eye in this case, may provide an
49 advantage in minimizing systemic side effects. This is of particular interest as the on-target
50 systemic toxicity of VEGFR-2 inhibitors has been well established, and thus may be a barrier to
51 systemic use of such therapy in the treatment of AMD. This data may support the potential
52
53
54
55
56
57
58
59
60

1
2
3 clinical utility of systemically administered VEGFR-2 inhibitors with preferential ocular
4 distribution as a therapy for wet AMD. A similar strategy may be applicable to other disease
5
6 indications that would benefit from local drug distribution to limit systemic toxicity.
7
8
9

10 11 12 13 AUTHOR INFORMATION

14 15 **Corresponding Author**

16
17 *Erik L. Meredith. Novartis Institutes for Biomedical Research, Global Discovery Chemistry,
18
19 100 Technology Square, Cambridge MA 02139. erik.meredith@novartis.com.
20
21

22 23 **Present Addresses**

24
25
26 †N.M.: Raze Therapeutics, 400 Technology Square, Cambridge, MA 02139.

27
28 ‡J.K.: Department of Ophthalmology and Vision Science, University of Toronto, and Department
29 of Vision Sciences, Toronto Western Research Institute, 399 Bathurst Street, Toronto, Ontario
30 M5T 2S8, Canada.

31
32 †K.M.: My Health Partners, 39 Pleasant Blvd, Toronto, ON, M4T 1K2, Canada.

33
34 †L.J.: Coditas Group, 125 Westbourne Terrace, Brookline, 02446.

35
36 †N. J.: Mitobridge, Inc. 1030 Massachusetts Avenue, Suite 200, Cambridge, MA 02138.

37
38 †G.A.: Kalexsyn, 4502 Campus Drive, Kalamazoo, MI, 49008.

39
40 †L.H.: Sensirion, Laubisruetistrasse, 508712 Staefa ZH, Switzerland.

41
42 †V.H.: AstraZeneca Neuroscience Innovative Medicines, 141 Portland Street, 10th Floor,
43
44 Cambridge, MA, 02139.

45
46 †C.R.: School of Biological Science, Nanyang Technological University, 60 Nanyang Drive,
47
48 Singapore, 637551.

49
50 †Y.Z.: 4237 Time Square Blvd, Dublin, Ohio 43016.

51 52 53 **Author Contributions**

54 55 56 57 58 59 60 ACKNOWLEDGMENT

1
2
3 The authors acknowledge the contribution of the Novartis Institute for Biomedical Research
4 Analytical Sciences group and the Novartis Institute for Biomedical Research Metabolism and
5 Pharmacokinetics group for support in generating the analytical detail for the compounds
6 described herein.
7
8
9
10
11

12 ABBREVIATIONS

13
14
15
16 TLC, thin layer chromatography; VEGF, vascular endothelial growth factor; AMD, age-related
17 macular degeneration; ADME, absorption distribution metabolism excretion CNV, choroidal
18 neovascularization; PEC, posterior eye cup; p.o., oral; i.v., intravenous; i.v.t., intravitreal;
19
20
21
22
23
24
25
26
27
28
29
30
31
32
33
34
35
36
37
38
39
40
41
42
43
44
45
46
47
48
49
50
51
52
53
54
55
56
57
58
59
60

ETDRS, Early Treatment of Diabetic Retinopathy Study; WFI, water for injection; MC, methylcellulose; CMC, carboxymethylcellulose; DN, dose normalized.

REFERENCES

- ¹ CATT Research Group. Ranibizumab and Bevacizumab for Neovascular Age-Related Macular Degeneration. *N. Engl. J. Med.* **2011**, *364*, 1897-1908.
- ² Brown, D. M., Kaiser, P. K., Michels, M., Soubrane, G., Heier, J. S., Kim, R. Y., Sy, J. P., Schneider, S. Ranibizumab versus verteporfin for neovascular age-related macular degeneration. *N. Engl. J. Med.* **2006**, *355*, 1432-1444.
- ³ Ferrara, N., Davis-Smyth, T. The biology of vascular endothelial growth factor. *Endocr. Rev.* **1997**, *18*(1), 4-25.
- ⁴ Bates, D. O., Curry, F. E. Vascular endothelial growth factor increases microvascular permeability via a Ca²⁺-dependent pathway. *Am. J. Physiol.* **1997**, *273*(2 Pt 2), H687-694.

1
2
3
4
5
6
7
8
9
10
11
12
13
14
15
16
17
18
19
20
21
22
23
24
25
26
27
28
29
30
31
32
33
34
35
36
37
38
39
40
41
42
43
44
45
46
47
48
49
50
51
52
53
54
55
56
57
58
59
60

⁵ Gao, H., Qiao, X., Gao, R., Mieler, W. F., McPherson, A. R., Holz, E. R. Intravitreal triamcinolone does not alter basal vascular endothelial growth factor mRNA expression in rat retina. *Vision Res.* **2004**, *44*(4), 349-356.

⁶ Lopez, P. F., Sippy, B. D., Lambert, H. M., Thach, A. B., Hinton, D. R. Transdifferentiated retinal pigment epithelial cells are immunoreactive for vascular endothelial growth factor in surgically excised age-related macular degeneration-related choroidal neovascular membranes. *Invest. Ophthalmol. Vis. Sci.* **1996**, *37*(5), 855-868.

⁷ Aiello, L. P., Avery, R. L., Arrigg, P. G., Keyt, B. A., Jampel, H. D., Shah, S. T., Pasquale, L. R., Thieme, H., Iwamoto, M. A., Park, J. E., Nguyen, H. V., Aiello, L. M., Ferrara, N., King, G. L. Vascular endothelial growth factor in ocular fluid of patients with diabetic retinopathy and other retinal disorders. *N. Engl. J. Med.* **1994**, *331*(22), 1480-1487.

⁸ Nguyen, Q. D., Tatlipinar, S., Shah, S. M., Haller, J. A., Quinlan, E., Sung, J., Zimmer-Galler, I., Do, D. V., Campochiaro, P. A. Vascular endothelial growth factor is a critical stimulus for diabetic macular edema. *Am. J. Ophthalmol.* **2006**, *142*(6), 961-9.

⁹ Terman, B. I., Dougher-Vermazen, M., Carrion, M. E., Dimitrov, D., Armellino, D. C., Gospodarowicz, D., Böhlen, P. Identification of the KDR tyrosine kinase as a receptor for vascular endothelial cell growth factor. *Biochem. Biophys. Res. Commun.* **1992**, *187*(3), 1579-1586.

¹⁰ Shalaby, F., Rossant, J., Yamaguchi, T. P., Gertsenstein, M., Wu, X. F., Breitman, M. L., Schuh, A. C. Failure of blood-island formation and vasculogenesis in Flk-1-deficient mice. *Nature* **1995**, *376*(6535), 62-66.

¹¹ Matsumoto, T., Claesson-Welsh, L. VEGF receptor signal transduction. *Sci. STKE* **2001**, *2001*(112), re21.

1
2
3 ¹² Keefe, D., Bowen, J., Gibson, R., Tan, T., Okera, M., Stringer, A. Noncardiac vascular
4 toxicities of vascular endothelial growth factor inhibitors in advanced cancer: a review.
5
6

7
8 *Oncologist* **2011**, 16(4), 432-444.
9

10 ¹³ Boyer, S. J. Small molecule inhibitors of KDR (VEGFR-2)kinase: an overview of structure
11 activity relationships. *Curr. Top. Med. Chem.* **2002**, 2, 973-1000.
12
13

14 ¹⁴ Schenone, S., Bondavalli, F., Botta, M. Antiangiogenic agents: an update on small molecule
15 VEGFR inhibitors. *Curr. Med. Chem.* **2007**, 14, 2495-2516.
16
17

18 ¹⁵ Schenone, S., Musumeci, F., Radi, M., Brullo, C. Vascular Endothelial Growth Factor
19 (VEGF) Receptors: Drugs and New Inhibitors. *J. Med. Chem.* **2012**, 55, 10797-10822 and
20 references therein.
21
22

23 ¹⁶ Diago, T., Pulido, J. S., Molina, J. R., Collett, L. C., Link, T. P., and Ryan, E. H., Jr.
24 Ranibizumab combined with low-dose sorafenib for exudative age-related macular degeneration.
25 *Mayo Clin Proc* **2008**, 83, 231-234.
26
27

28 ¹⁷ Kernt, M., Staehler, M., Stief, C., Kampik, A., and Neubauer, A. S. Resolution of macular
29 oedema in occult choroidal neovascularization under oral Sorafenib treatment. *Acta Ophthalmol*
30 **2008**, 86, 456-458.
31
32

33 ¹⁸ Amparo, F., Sadrai Z., Jin, Y., Alfonso-Bartolozzi, B., Wang, H., Shikari, H., Ciolino, J. B.,
34 Chodosh, J., Jurkunas, U., Schaumberg, D. A., Dana, R. Safety and Efficacy of the Multitargeted
35 Receptor Kinase Inhibitor Pazopanib in the Treatment of Corneal Neovascularization. *Invest.*
36 *Ophthalmol. Vis. Sci.* **2013**, 54, 537-544.
37
38

39 ¹⁹ Kwak, N., Okamoto, N., Wood, J. M., and Campochiaro, P. A. VEGF is major stimulator in
40 model of choroidal neovascularization. *Invest. Ophthalmol. Vis. Sci.* **2000**, 41, 3158-3164.
41
42
43
44
45
46
47
48
49
50
51
52

1
2
3 ²⁰ Bold, G., Capraro, H-G., Caravatti, G., Floersheimer, A., Furet, P., Manley, P., Vaupel, A.,
4
5 Pissot Soldermann, C., Gessier, F., Schnell, C., Littlewood-Evans, A. J., Kapa, P. K., Bajwa, J.
6
7 S., Jiang, X. Preparation of Bicyclic Amides as Kinase Inhibitors. *PCT Int. Appl.* (2006), WO
8
9 2006059234.

10
11
12 ²¹ Bold, G., Vaupel, A., Lang, M. Heterobicyclic carboxamides as protein kinase inhibitors and
13
14 their preparation, pharmaceutical compositions and use in the treatment of proliferative diseases.
15
16 *PCT Int. Appl.* (2008), WO 2008009487.

17
18
19 ²² Wan, Z-K., Wacharasindhu, S., Levins, C. G., Lin, M., Tabei, K., Mansour, T. S. The Scope
20
21 and Mechanism of Phosponium-Mediated S_NAr Reactions in Heterocyclic Amides and Ureas
22
23 *J. Org. Chem.*, 2007, 72 (26), 10194–10210.

24
25 ²³ Ji, N., Meredith, E. L., Liu, D., Adams, C. M., Artman, G. D., Jendza, K. C., Ma, F.,
26
27 Mainolfi, N., Powers, J. J., Zhang, C. Synthesis of 1-substituted-3-aminopyrazoles *Tetrahedron*
28
29 *Lett.* 2010, 51, 6799-6801.

30
31 ²⁴ Johnson, L., Powers, J., Ma, M., Jendza, K., Wang, B., Meredith E. L., Mainolfi, N. A
32
33 Reliable Synthesis of 3-Amino-5-Alkyl and 5-Amino-3-Alkyl Isoxazoles. *Synthesis* 2013, 45,
34
35 171-173.

36
37 ²⁵ (a) Jones, K. A., Garbati, N., Zhang, H., Large, C. H. Automated patch clamping using the
38
39 QPatch. *Methods Mol. Biol.* 2009, 565, 209–223. (b) Kutchinsky, J., Friis, S., Asmild, M.,
40
41 Taboryski, R., Pedersen, S., Vestergaard, R. K., Jacobsen, R. B., Krzywkowski, K., Schroder, R.
42
43 L., Ljungstrom, T., Helix, N., Sorensen, C. B., Bech, M., Willumsen, N. J. Characterization of
44
45 potassium channel modulators with QPatch automated patch-clamp technology: system
46
47 characteristics and performance. *Assay Drug Dev. Technol.* 2003, 1, 685–693.
48
49
50
51
52
53
54
55
56
57
58
59
60

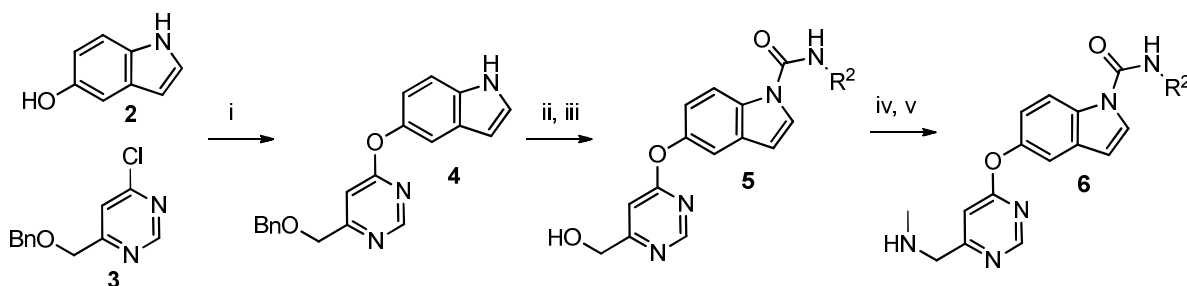
²⁶Zhou, L., Yang, L., Tilton, S., Wang, J. Development of a High Throughput Equilibrium Solubility Assay Using Miniaturized Shake-Flask Method in Early Drug Discovery. *J. Pharm. Sci.* **2007**, *96*, 3052-3071.

²⁷Takahashi, K., Saishin, Yo., Saishin, Yu., King, A. G., Levin, R., Campochiaro, P. A. Suppression and Regression of Choroidal Neovascularization by the Multitargeted Kinase Inhibitor Pazopanib. *Arch. Ophthalmol.* **2009**, *127*, 494-499.

²⁸Connolly, T. J., Matchett, M., Sarma, K. Process Development and Scale-up of a Selective α_1 -Adrenoreceptor Antagonist. *Org. Proc. Res. Dev.* **2005**, *9*, 8087.

²⁹Seelen, W., Schäfer, M., Ernst, A. Selective ring N-protection of aminopyrazoles. *Tetrahedron. Lett.* **2003**, *44*, 4491-4493.

Scheme 1^a



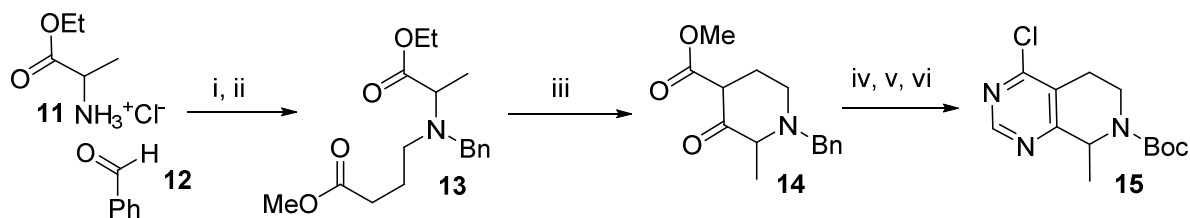
^aReagents and Conditions: (i) DBU, CH₃CN, 75%; (ii) NaH, R²NCO, DMF, -50 °C to rt, 88%; (iii) TFA, 100 °C, 74%; (iv) Ms₂O, pyridine, THF; (v) CH₃NH₂, MeOH, 54%, 2 steps.

Scheme 2^a



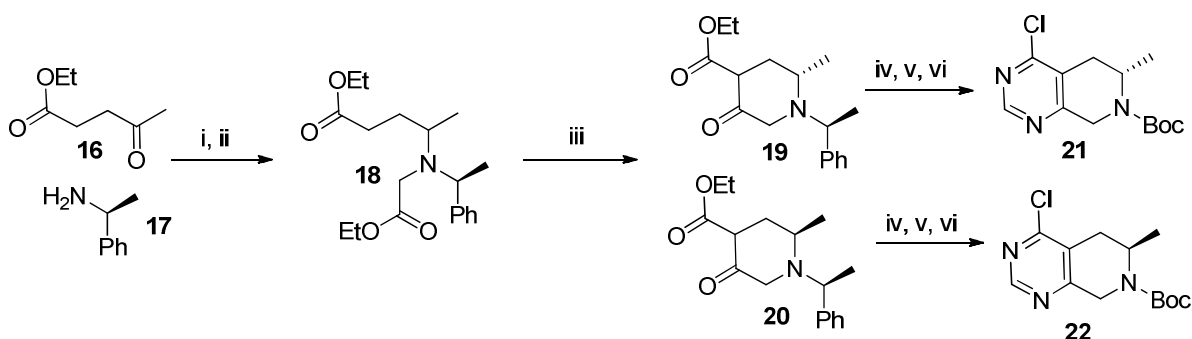
^aReagents and Conditions: (i) formamidine acetate, EtONa, EtOH, reflux, 90%; (ii) Pd/C, Boc₂O, MeOH/THF; (iii) CCl₄, PPh₃, DCE, reflux, 80%, 2 steps.

Scheme 3^a



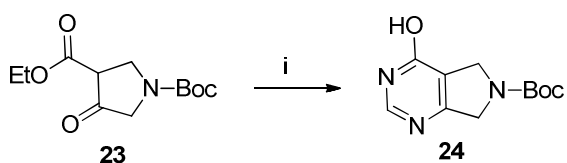
^aReagents and Conditions: (i) **11**, **12**, NaBH(OAc)₃, TEA, DCE; (ii) ethyl oxobutanoate, NaBH(OAc)₃, DCE; (iii) *t*BuOK, toluene; (iv) formamidine acetate, EtONa, EtOH, reflux, 36% 4 steps; (v) Pd/C, Boc₂O, MeOH; (vi) CCl₄, PPh₃, DCE, reflux 57%, 2 steps.

Scheme 4^a

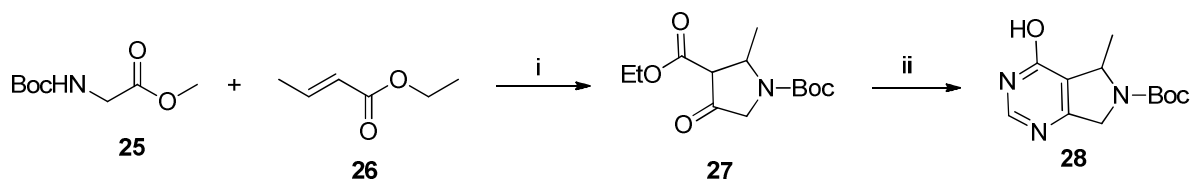


^aReagents and Conditions: (i) **16**, **17**, NaBH(OAc)₃, DCE; (ii) ethyl glyoxylate, NaBH(OAc)₃, DCE; (iii) *t*BuOK, toluene, 50-70%, 3 steps; (iv) formamidine acetate, EtONa, EtOH, reflux, 93%; (v) Pd/C, Boc₂O, EtOH, 80%, 2 steps; (vi) CCl₄, PPh₃, DCE, reflux, 51%.

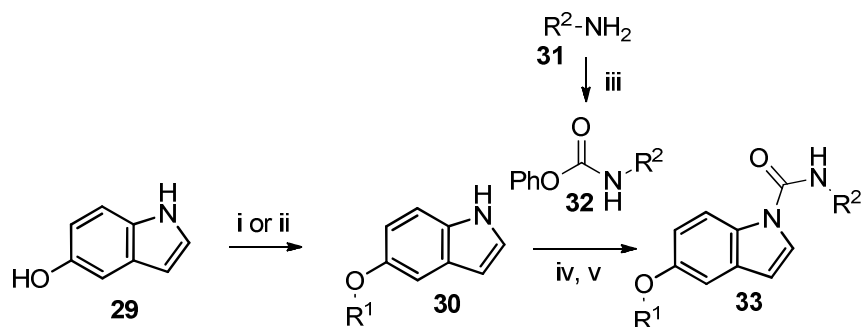
Scheme 5^a



^aReagents and Conditions: (i) formamidine acetate, EtONa, EtOH, reflux, 24%.

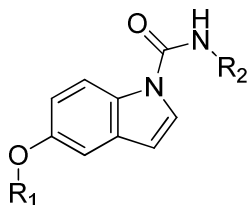
Scheme 6^a

^aReagents and Conditions: (i) NaH, toluene, 0 °C to rt; (ii) formamidine acetate, EtONa, EtOH, reflux, ~20%.

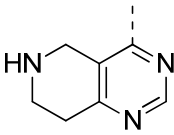
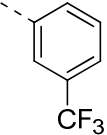
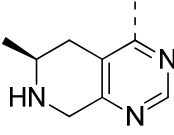
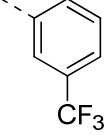
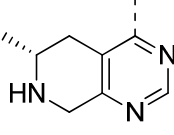
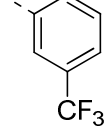
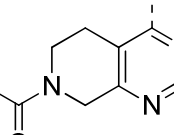
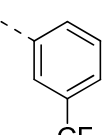
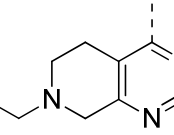
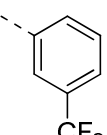
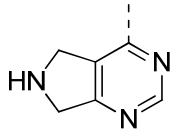
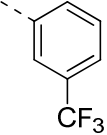
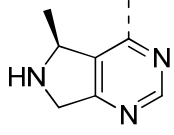
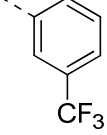
Scheme 7^a

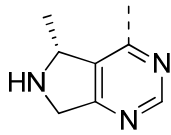
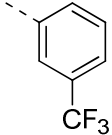
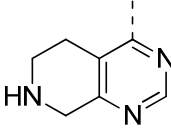
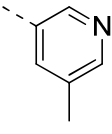
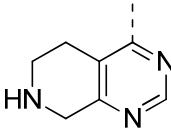
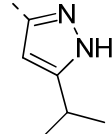
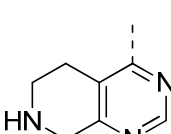
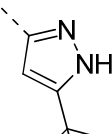
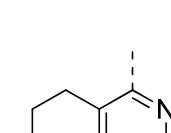
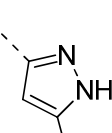
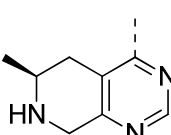
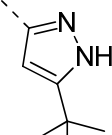
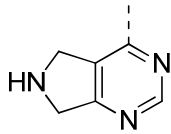
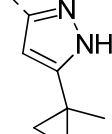
^aReagents and Conditions: (i) **10**, **15**, **21**, or **22**, DBU, CH₃CN, reflux, 90%; (ii) **24** or **28**, PyBop, acetonitrile, DBU, 64%; (iii) **25**, phenyl chloroformate, pyridine, 86%; (iv) **32** or R²NCO, NaH, THF, 0 °C-rt, 50%; (v) TFA, DCM, 92%.

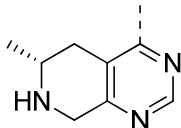
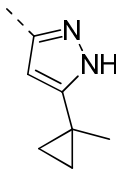
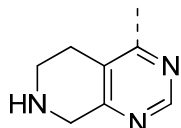
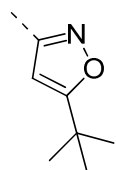
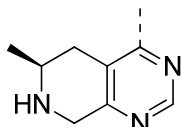
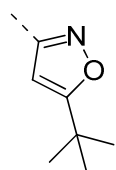
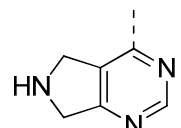
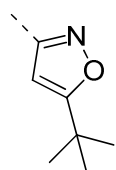
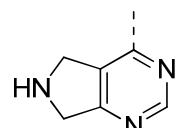
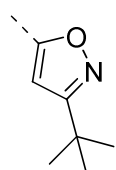
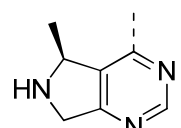
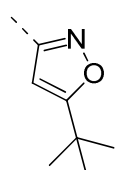
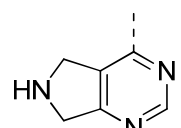
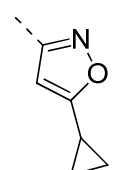
Table 1. In vitro inhibition data (KDR biochemical; BaF3 cellular) and in vivo (% inhibition of mouse CNV) for selected compounds.

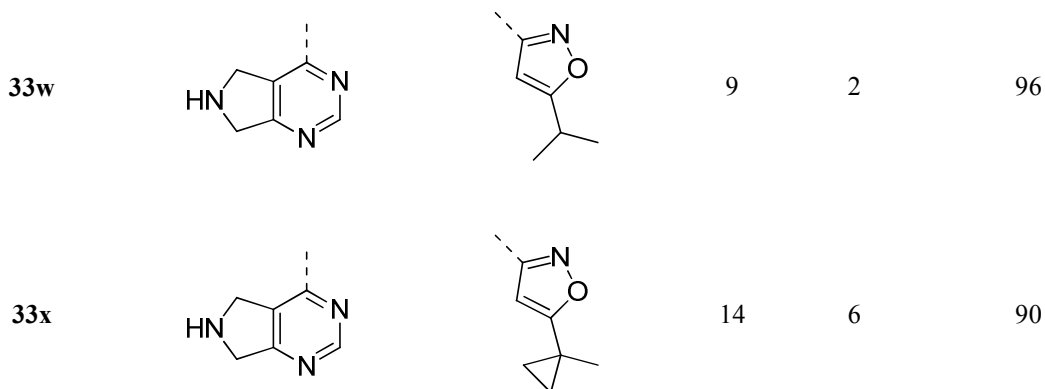


CMPD	R ₁	R ₂	KDR IC ₅₀ (nM) ^a	BaF3 IC ₅₀ (nM) ^a	mCNV % inhibition @ 10 mg/kg qd ^b
1			17	--	44
5a			13	4	45
6a			8	11	67
6b			5	66	92
33a			22	10	87

1						
2						
3						
4						
5						
6	33b			18	81	0
7						
8						
9						
10						
11						
12	33c			24	60	96
13						
14						
15						
16						
17						
18						
19	33d			23	109	58
20						
21						
22						
23						
24						
25						
26	33e			7	--	0
27						
28						
29						
30						
31						
32						
33						
34	33f			10	10	81
35						
36						
37						
38						
39						
40						
41						
42	33g			29	0.4	68
43						
44						
45						
46						
47						
48	33h			16	118	41
49						
50						
51						
52						
53						
54						
55						
56						
57						
58						
59						
60						

1						
2						
3						
4						
5						
6	33i			17	--	0
7						
8						
9						
10						
11	33j			280	1922	--
12						
13						
14						
15						
16						
17						
18	33k			6	3	0
19						
20						
21						
22						
23						
24						
25						
26	33l			8	1	0
27						
28						
29						
30						
31						
32						
33	33m			5	3	64
34						
35						
36						
37						
38						
39						
40						
41	33n			8	0.9	67
42						
43						
44						
45						
46						
47						
48	33o			< 3	0.5	43
49						
50						
51						
52						
53						
54						
55						
56						
57						
58						
59						
60						

1						
2						
3						
4						
5						
6						
7	33p			8	0.9	48
8						
9						
10						
11						
12						
13	33q			30	40	83
14						
15						
16						
17						
18						
19						
20						
21	33r			30	4	96
22						
23						
24						
25						
26						
27						
28						
29	33s			9	59	83
30						
31						
32						
33						
34						
35						
36	33t			114	167	58
37						
38						
39						
40						
41						
42						
43						
44	33u			22	8	33
45						
46						
47						
48						
49						
50						
51	33v			41	26	98
52						
53						
54						
55						
56						
57						
58						
59						
60						



18 ^aValues are mean of at least two experiments (IC₅₀, nM). ^bCompounds dosed q.d. orally as
19 0.5% CMC/0.1% tween 80.
20
21
22

23 **Table 2.** Comparison of aqueous solubility for selected VEGFR-2 inhibitors.
24

CMPD	aq sol pH 6.8 (μM) ^a
1	5
6a	64
33a	84
33f	<5
33j	190
33k	833
33l	682
33m	252
33n	450
33o	489
33q	167
33r	126
33s	20
33t	232
33v	110
33w	37

25
26
27
28
29
30
31
32
33
34
35
36
37
38
39
40
41
42
43
44
45
46
47
48
49
50
51
52 ^a Aqueous high-throughput equilibrium solubility (see ref. 24).
53
54
55
56
57
58
59
60

Table 3. Comparison of hERG activity for selected VEGFR-2 inhibitors.

CMPD	hERG IC ₅₀ (nM) ^a
6b	5800
33a	8900
33c	10700
33g	15600
33m	>30000
33n	27400
33q	7000
33r	11100
33s	23500
33v	>30000

^a Automated Q-patch assay.**Table 4.** Dose response inhibition of laser induced choroidal neovascularization for selected VEGFR-2 inhibitors.

CMPD	mouse ^a		rat ^b	
	ED ₅₀ (mg/kg)	ED ₉₀ (mg/kg)	ED ₅₀ (mg/kg)	ED ₉₀ (mg/kg)
33c	3.6	8.5	--	--
33g	6.9	31	--	--
33n	3.4	19.6	2.9	14.6
33v	1.8	4.8	0.7	2.7
33m	7.8	25.3	2.7	13.6

^aCompounds dosed q.d. orally as 0.5% MC/0.1% tween 80, WFI 7 days. ^bCompounds dosed q.d. orally as 0.5% CMC/0.1% tween 80, WFI 14 days.

Table 5. Dose normalized (DN) exposure in selected tissues from Brown Norway rat for selected VEGFR-2 inhibitors **33n**^a, **33m**^b and **33v**^c.

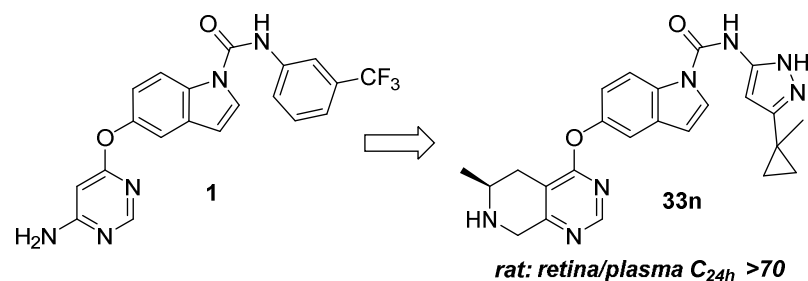
Tissue	compd	DNAUC _{PO 0-24h} (nM* <i>h</i> /mg/kg)	DNC _{Max} (nM/mg/kg)	DNC _{24h} (nM/mg/kg)
plasma	33n	598	68	1.6
	33v	15014	3225	6
	33m	166	33	0.7
retina	33n	3215	170	122
	33v	2692	337	65
	33m	310	15	13
PEC	33n	22266	1067	1067
	33v	92954	5293	3344
	33m	2386	110	102

Each compound was dosed orally as a suspension 0.5% MC/0.1% tween 80, WFI at the following doses: ^a6 mg/kg (ED₅₀ = 3.0 mg/kg); ^b6 mg/kg (ED₅₀ = 2.7 mg/kg); ^c2 mg/kg (ED₅₀ = 0.7mg/kg). PEC = posterior eye cup (retinal pigment epithelium/choroid/sclera complex).

Table 6. PK-ADME parameters for selected VEGFR-2 inhibitors.^a

Parameter	33n ^{b,d,f}	33v ^{b,e,f}	33m ^{c,d,f}
AUC _{PO 0-8h} (μM* <i>h</i>)	2488	29393	1121
CL (mL/min/kg)	27	6	165
V _{dss} (L / kg)	5.6	0.5	22
t _{1/2} (h)	2.3	1.2	2.7
C _{max} (nM)	514	11003	505
F (%)	81	100	51

^aBrown Norway rat PK. Animals were dosed either i.v. (1 mg/kg, n = 2) or p.o. (3^b or 10^c mg/kg, n = 3). ^di.v. dose: 10% NMP, 15% PG, 4% cremophorEL, PBS. ^ei.v. dose: 10% NMP, 30% PEG 300, 60% WFI. ^fp.o. dose: 0.5% MC/0.1% tween 80, WFI PK parameters derived from p.o. dosing, and are reported as mean ± SD.



Chemistry.

General. NMR spectra were recorded on a Bruker Avance II 400 MHz spectrometer. All chemical shifts are reported in parts per million (δ) relative to tetramethylsilane. The following abbreviations are used to denote signal patterns: s = singlet, d = doublet, t = triplet, m =

1
2
3
4
5
6
7
8
9
10
11
12
13
14
15
16
17
18
19
20
21
22
23
24
25
26
27
28
29
30
31
32
33
34
35
36
37
38
39
40
41
42
43
44
45
46
47
48
49
50
51
52
53
54
55
56
57
58
59
60

multiplet, and br = broad. Flash chromatography was conducted using Grade 60 230-400 mesh silica gel from Fisher Chemical (S825-1) or by utilizing the CombiFlash Companion from Teledyne Isco, Inc. and RediSep® Rf disposable normal phase silica gel columns (4-300 g). Thin layer chromatography was performed using 2.5 x 7.5 cm glass-backed TLC Silica Gel 60 F₂₅₄ plates from EMD Chemicals, Inc. (15341-1) and visualized by UV light. HPLC purifications were performed on a Gilson preparative HPLC system controlled by Unipoint software using X-Bridge™ Phenyl, C8, C18, or RP18 30 x 50 mm columns with 5 μm particle size. The purity of all compounds was ≥ 95%, unless otherwise noted. Low-resolution mass spectra were recorded using an Agilent 1100 series LC-MS spectrometer.

5-(6-Benzyloxymethyl-pyrimidin-4-yloxy)-1H-indole (4). **5-(6-Benzyloxymethyl-pyrimidin-4-yloxy)-1H-indole (4).** 5-Hydroxy indole **2** (5 g, 37.6 mmol) was added in one portion to a solution of 4-(benzyloxymethyl)-6-chloropyrimidine **3** (8.81 g, 37.6 mmol) and DBU (5.66 mL, 37.6 mmol) in ACN (107 mL) at room temperature. This was stirred overnight for 20 hours. The reaction was concentrated and purified via FCC (12-100% EtOAc/heptane) to obtain the title compound (9.37 g, 28.3 mmol, 75 % yield). MS (ESI) *m/z* 447.0 (M+1); ¹H NMR (400 MHz, DMSO-d₆) δ 11.11 - 11.44 (m, 1 H), 8.58 - 8.82 (m, 1 H), 7.41 - 7.51 (m, 2 H), 7.34 - 7.39 (m, 1 H), 7.21 - 7.32 (m, 5 H), 6.88 - 6.94 (m, 2 H), 6.42 - 6.50 (m, 1 H), 4.52 - 4.64 (m, 4 H).

5-(6-Hydroxymethyl-pyrimidin-4-yloxy)-indole-1-carboxylic acid (4-fluoro-3-trifluoromethyl-phenyl)-amide (5). To NaH (255 mg, 6.37 mmol) in 40 mL DMF at 0°C under nitrogen, was added a solution of 5-(6-(benzyloxymethyl)pyrimidin-4-yloxy)-1H-indole (960mg, 2.90 mmol) in 5 ml DMF and stirred at 0°C 0.5h. The reaction was then cooled to -

50°C, followed by addition of 1-fluoro-4-isocyanato-2-(trifluoromethyl)benzene (0.454 ml, 3.19 mmol) in 5 mL DMF. The cold bath was removed and the reaction allowed to warm to RT.

After 3h the reaction was quenched with NH₄Cl, extracted 2x EtOAc, and the combined organics washed combined organics with H₂O (3x), brine, dried over Na₂SO₄ and concentrated.

The residue was then purified via FCC (1-50% EtOAc:CH₂Cl₂) to obtain 5-((6-((benzyloxy)methyl)pyrimidin-4-yl)oxy)-N-(4-fluoro-3-(trifluoromethyl)phenyl)-1H-indole-1-carboxamide (1.36 g, 2.54 mmol, 88% yield). MS (ESI) *m/z* 537.0 (M+1); ¹H NMR (400 MHz, DMSO-d₆) δ 10.40 (s, 1 H), 8.69 (s, 1 H), 8.30 (d, *J*=8.84 Hz, 1 H), 8.07 - 8.19 (m, 2 H), 7.96 - 8.06 (m, 1 H), 7.58 (t, *J*=9.85 Hz, 1 H), 7.52 (d, *J*=2.27 Hz, 1 H), 7.24 - 7.40 (m, 5 H), 7.17 (dd, *J*=8.97, 2.40 Hz, 1 H), 7.02 (s, 1 H), 6.82 (d, *J*=3.79 Hz, 1 H), 4.61 (d, *J*=8.84 Hz, 4 H).

A solution of 5-((6-((benzyloxy)methyl)pyrimidin-4-yl)oxy)-N-(4-fluoro-3-(trifluoromethyl)phenyl)-1H-indole-1-carboxamide (1.48 g, 2.76 mmol) in TFA (15 mL) was heated at 100 °C for 4 h before concentrating and absorbing onto silica to purify via FCC 10-100% EtOAc:CH₂Cl₂ 10CV, then 100% EtOAc to provide the title compound **5** (0.915 g, 2.052 mmol, 74% yield). MS (ESI) *m/z* 447.0 (M+1); ¹H NMR (400 MHz, DMSO-d₆) δ 10.40 (s, 1 H), 8.65 (d, *J*=1.01 Hz, 1 H), 8.29 (d, *J*=9.09 Hz, 1 H), 8.09 - 8.12 (m, 2H), 8.99 - 8.04 (m, 1 H), 7.58 (t, *J*=9.60 Hz, 1 H), 7.51 (d, *J*=2.53 Hz, 1 H), 7.16 (dd, *J*=8.84, 2.53 Hz, 1 H), 6.99 (d, *J*=1.01 Hz, 1 H), 6.82 (d, *J*=3.79 Hz, 1 H), 5.61 (t, *J*=5.05 Hz, 1 H), 4.52 (d, *J*=5.05 Hz, 2 H).

5-(6-Methylaminomethyl-pyrimidin-4-yloxy)-indole-1-carboxylic acid (4-fluoro-3-trifluoromethyl-phenyl)-amide (6b). To a solution of 5-(6-hydroxymethyl-pyrimidin-4-yloxy)-indole-1-carboxylic acid (4-fluoro-3-trifluoromethyl-phenyl)-amide **5** (260 mg, 0.6 mmol), methanesulfonic anhydride (240 mg, 1.4 mmol), and THF (15 mL) was added pyridine (0.2 mL).

1
2
3 The mixture was stirred at rt for 0.5 h before being filtered. The filtrate was used in the next step
4
5 without purification. MS (ESI) m/z 525.0 (M+1).
6
7

8 To a solution of 5-(6-methanesulfonylmethyl-pyrimidin-4-yloxy)-indole-1-carboxylic acid (4-
9
10 fluoro-3-trifluoromethyl-phenyl)-amide ((270 mg, 0.515 mmol) was added methyl amine (8 mL,
11
12 2.0 M in methanol). The mixture was stirred at room temperature for 16 h, then concentrated
13
14 under reduced pressure. The residue was diluted with EtOAc and washed with water and brine.
15
16 The organic layer was removed, dried, and concentrated. The residue was then separated by
17
18 FCC (MeOH with 1% NH₄OH/DCM from 0% to 10%) to give the title compound **6b** (127 mg,
19
20 0.276 mmol, 54%). MS (ESI) m/z 460.1 (M+1); ¹H NMR (400 MHz, methanol-d₄) δ 8.65 (d,
21
22 $J=1.01$ Hz, 1 H), 8.35 (d, $J=8.84$ Hz, 1 H), 8.04 (dd, $J=6.19, 2.65$ Hz, 1 H), 7.90 – 7.94 (m, 2 H),
23
24 7.41 (d, $J=2.27$ Hz, 1 H), 7.35 (t, $J=9.60$ Hz, 1 H), 7.11 (dd, $J=8.97, 2.40$ Hz, 1 H), 7.00 (s, 1 H),
25
26 6.74 (d, $J=3.79$ Hz, 1 H), 3.82 (s, 2 H), 2.43 (s, 3 H).
27
28
29
30
31
32

33 **5-(6-Methylaminomethyl-pyrimidin-4-yloxy)-indole-1-carboxylic acid (3-trifluoromethyl-
34
35 phenyl)-amide (6a)**. Prepared as described for **6b**. MS (ESI) m/z 442.1 (M+1); ¹H NMR (400
36
37 MHz, methanol-d₄) δ 8.64 (s, 1 H), 8.34 (d, $J=9.09$ Hz, 1 H), 8.05 (s, 1 H), 7.93 (d, $J=3.79$ Hz, 1
38
39 H), 7.89 (d, $J=8.08$ Hz, 1 H), 7.56 (t, $J=7.96$ Hz, 1 H), 7.40 – 7.46 (m, 2 H), 7.10 (dd, $J=8.97,$
40
41 2.40 Hz, 1 H), 6.99 (s, 1 H), 6.73 (d, $J=3.79$ Hz, 1 H), 3.77 (s, 2 H), 2.40 (s, 3 H).
42
43
44
45

46 **4-Chloro-5,8-dihydro-6H-pyrido[3,4-*d*]pyrimidine-7-carboxylic acid *tert*-butyl ester (8)**.
47
48 7-Benzyl-5,6,7,8-tetrahydro-3H-pyrido[3,4-*d*]pyrimidin-4-one²⁸ (36.9 g, 153 mmol) and BOC
49
50 anhydride (40.1 g, 184 mmol) were taken up in MeOH (600 mL). The vessel was purged with
51
52 argon and palladium on carbon (10% w/w; wet) (5.0 g) was added. The contents were then
53
54 stirred under a hydrogen atmosphere (1 atm) for 18 h. At that time the suspension was filtered
55
56
57
58
59
60

1
2
3 over Celite® and the resulting solution was concentrated to give the title compound which was
4
5 taken to the next step without further purification. MS (ESI) m/z 252.0 (M+1); ^1H NMR (400
6
7 MHz, DMSO- d_6) δ 12.41 (s, 1H), 8.04 (s, 1H), 4.22 (s, 2H), 3.51 (app t, J = 5.7 Hz, 2H), 2.40
8
9 (app t, J = 5.7 Hz, 2H), 1.42 (s, 9H).

10
11
12 Triphenylphosphine (17.3 g, 66.1 mmol) was added to a solution of 4-oxo-4,5,6,8-tetrahydro-
13
14 3H-pyrido[3,4-*d*]pyrimidine-7-carboxylic acid *tert*-butyl ester (8.30 g, 33.0 mmol), CCl_4 (9.6
15
16 mL, 99 mmol), and 1,2-dichloroethane (250 mL). The solution was heated at 70 °C for 2.5 h.
17
18 The solution was concentrated in vacuo to about 50 mL. The contents of the flask were then
19
20 filtered over a silica gel plug eluting with 60% EtOAc/heptane. The residue following
21
22 concentration was then further separated via flash chromatography (10-30% EtOAc/heptane) to
23
24 give the title compound **8** (7.09 g, 26.3 mmol, 80 %). MS (ESI) m/z 270.0 & 272.0 (M+1); ^1H
25
26 NMR (400 MHz, chloroform-*d*) δ 8.79 (s, 1 H), 4.65 (s, 2 H), 3.74 (t, J = 5.8 Hz, 2 H), 2.87 (t,
27
28 J = 5.8 Hz, 2 H), 1.49 (s, 9 H).
29
30
31
32
33
34

35 ***tert*-Butyl 4-chloro-7,8-dihydropyrido[4,3-*d*]pyrimidine-6(5H)-carboxylate (10)**. Prepared
36
37 as described for **8**. MS (ESI) m/z 270.0 & 271.9 (M+1); ^1H NMR (400 MHz, chloroform-*d*) δ
38
39 8.79 (s, 1H), 4.58 (s, 2H), 3.76 (t, J = 5.9 Hz, 2H), 2.97 (t, J = 5.8 Hz, 2H), 1.50 (s, 9H).
40
41
42

43 **4-[Benzyl-(1-ethoxycarbonyl-ethyl)-amino]-butyric acid methyl ester (13)**. Ethyl alanine
44
45 hydrochloride (5.5 g, 36.8 mmol), benzaldehyde (7.9 mL, 77.8 mmol), TEA (10.8 mL, 77.8
46
47 mmol) and $\text{NaBH}(\text{OAc})_3$ (16.5 g, 77.8 mmol) were taken up in 1,2-DCE (200 mL) and stirred at
48
49 rt for 4 h. The reaction was then partitioned between DCM and saturated aqueous NaHCO_3 .
50
51 The organic layer was removed, dried over anhydrous Na_2SO_4 , and concentrated in vacuo. The
52
53 crude residue was used without further purification. MS (ESI) m/z 208.2 (M+1).
54
55
56
57
58
59
60

1
2
3 2-Benzylamino-propionic acid ethyl ester (1.4 g, 6.7 mmol), methyl oxo-butanoate (1.7 g, 13.5
4 mmol), TEA (1.9 mL, 13.5 mmol) and NaBH(OAc)₃ (2.9 g, 13.5 mmol) were taken up in 1,2-
5 DCE (35 mL) and stirred at rt for 4 h. The reaction was partitioned between DCM and saturated
6 aqueous NaHCO₃. The organic layer was removed, dried over anhydrous Na₂SO₄, and
7 concentrated in vacuo. The crude residue was used without further purification. MS (ESI) *m/z*
8 308.3 (M+1).
9
10
11
12
13
14
15
16
17

18 **1-Benzyl-2-methyl-3-oxo-piperidine-4-carboxylic acid methyl ester (14).** A mixture of 4-
19 [benzyl-(1-ethoxycarbonyl-ethyl)-amino]-butyric acid methyl ester (1.5 g, 4.9 mmol), potassium
20 *tert*-butoxide (906 mg, 8.9 mmol) and toluene (100 mL) was stirred at rt for 3 h. The mixture
21 was then partitioned between DCM and saturated aqueous NH₄Cl. The organic layer was
22 removed, dried over anhydrous Na₂SO₄, and concentrated. The crude residue was used without
23 further purification. MS (ESI) *m/z* 262.2 (M+1).
24
25
26
27
28
29
30
31
32
33

34 **4-Chloro-8-methyl-5,8-dihydro-6*H*-pyrido[3,4-*d*]pyrimidine-7-carboxylic acid *tert*-butyl**
35 **ester (15).** Prepared as described for **8**. MS (ESI) *m/z* 284.2 (M+H); ¹H NMR (400 MHz,
36 METHYLENE CHLORIDE-*d*₂) δ 8.67 (s, 1H), 5.24 – 5.23 (m, 2H), 5.05 (s, 1H), 4.26 (s, 1H),
37 2.97 (s, 1H), 1.42 (d, *J* = 6.9 Hz, 3H), 1.39 (s, 9H).
38
39
40
41
42
43
44
45

46 **Ethyl 4-((2-ethoxy-2-oxoethyl)((*S*)-1-phenylethyl)amino)pentanoate (18).** To a solution of
47 (*S*)-1-phenylethylamine (25.0 g, 206 mmol) and NaBH(OAc)₃ (65.6 g, 309 mmol) in 1,2-DCE
48 (500 mL) was added ethyl levulinate (29.4 mL, 206 mmol). The reaction was stirred at room
49 temperature for 16 h. The mixture was then partitioned between DCM and saturated aqueous
50 NaHCO₃. The organic layer was removed and the aqueous layer was extracted further with
51
52
53
54
55
56
57
58
59
60

1
2
3 DCM (2x). The combined organic layers were then dried over anhydrous Na₂SO₄, filtered, and
4 concentrated under reduced pressure. The crude ethyl 4-((*S*)-1-phenyl-ethyl)amino)pentanoate
5 was used without further purification. MS (ESI) *m/z* 250.2 (M+1).
6
7

8
9
10 To a solution of ethyl 4-((*S*)-1-phenylethylamino)pentanoate (51.4 g, 206 mmol) and
11 NaBH(OAc)₃ (65.5 g, 309 mmol) in 1,2-DCE (500 mL) was added ethyl glyoxylate (84 g, 412
12 mmol, 50% toluene solution). The reaction was stirred at room temperature for 18 h. The
13 mixture was then partitioned between DCM and saturated aqueous NaHCO₃. The organic layer
14 was removed and the aqueous layer was extracted further with DCM (2x). The combined
15 organic layers were then dried over anhydrous Na₂SO₄, filtered, and concentrated under reduced
16 pressure. The crude diastereomeric mixture of ethyl 4-((2-ethoxy-2-oxoethyl)((*S*)-1-
17 phenylethyl)amino)pentanoate (**18**) was used without further purification. MS (ESI) *m/z* 336.4
18 (M+1).
19
20
21
22
23
24
25
26
27
28
29
30
31

32
33 **(2*S*)-Ethyl 2-methyl-5-oxo-1-((*S*)-1-phenylethyl)piperidine-4-carboxylate (19) and (2*R*)-**
34 **Ethyl 2-methyl-5-oxo-1-((*S*)-1-phenylethyl)piperidine-4-carboxylate (20).** To a solution of
35 ethyl 4-((2-ethoxy-2-oxoethyl)((*S*)-1-phenylethyl)amino)pentanoate (44.5 g, 133 mmol) in
36 toluene (500 mL) was added KO^tBu (37.2 g, 332 mmol). After stirring for 3 h at room
37 temperature, the mixture was then partitioned between DCM and saturated aqueous NH₄Cl. The
38 organic layer was removed and the aqueous layer was extracted further with DCM (2x). The
39 combined organic layers were then dried over anhydrous Na₂SO₄, filtered, and then concentrated
40 under reduced pressure. The crude residue was purified via FCC (2.5% EtOAc/heptane) to give
41 the both of the title diastereomers (**19**: 20.6 g, 54%; **20**: 7.5 g, 19%). Analytical data for **19**: MS
42 (ESI) *m/z* 290.2 (M+1); ¹H NMR (400 MHz, chloroform-*d*) δ 11.81 (s, 1 H), 7.18 – 7.37 (m, 5
43 H), 4.16 – 4.27 (m, 2 H), 3.70 (q, *J*=6.6 Hz, 1 H), 3.27 – 3.38 (m, 1 H), 2.82 – 3.13 (m, 2 H),
44
45
46
47
48
49
50
51
52
53
54
55
56
57
58
59
60

1
2
3 2.53 (dd, $J=15.5, 5.2$ Hz, 1 H), 2.10 (dd, $J=15.5, 3.7$ Hz, 1 H), 1.33 (d, $J=6.6$ Hz, 3 H), 1.30 (t,
4
5 $J=7.1$ Hz, 3 H), 1.05 (d, $J=6.6$ Hz, 3 H). Analytical data for **20**: MS (ESI) m/z 290.2 (M+1); ^1H
6
7 NMR (400 MHz, CDCl_3) δ 11.94 (s, 1 H), 7.19 – 7.36 (m, 5 H), 4.13 – 4.29 (m, 2 H), 3.63 (q,
8
9 $J=6.6$ Hz, 1 H), 3.09 – 3.52 (m, 2 H), 2.94 – 3.05 (m, 1 H), 2.34 – 2.47 (m, 1 H), 1.94 (d, $J=15.4$
10
11 Hz, 1 H), 1.34 (d, $J=6.6$ Hz, 3 H), 1.28 (t, $J=7.2$ Hz, 3 H), 0.90 (d, $J=6.8$ Hz, 3 H).
12
13
14
15

16
17 **(S)-tert-Butyl 4-chloro-6-methyl-5,6-dihydropyrido[3,4-d]pyrimidine-7(8H)-carboxylate**

18
19 **(21)**. A combination of (2S)-Ethyl 2-methyl-5-oxo-1-((S)-1-phenylethyl)piperidine-4-
20
21 carboxylate **19** (20.6 g, 71.2 mmol), formamidine acetate (11.1 g, 107 mmol), and EtOH (250
22
23 mL) was treated with NaOEt solution (57.7 g, 178 mmol, 21% w/w EtOH solution) and then
24
25 heated at 90 °C for 4 h. At that point the solvent was removed under reduced pressure and the
26
27 residue was taken up in DCM and washed with sat aq NH_4Cl . The aqueous layer was further
28
29 extracted with DCM and the combined organic layers were then dried over sodium sulfate,
30
31 filtered and concentrated to give (S)-6-methyl-7-((S)-1-phenylethyl)-5,6,7,8-
32
33 tetrahydropyrido[3,4-d]pyrimidin-4(3H)-one, which was taken to the next step without further
34
35 purification. MS (ESI) m/z 270.1 (M+1).
36
37
38
39

40
41 To a mixture of (S)-6-methyl-7-((S)-1-phenylethyl)-5,6,7,8-tetrahydropyrido[3,4-d]pyrimidin-
42
43 4(3H)-one (20.0 g, 74.3 mmol), ammonium formate (23.4 g, 371 mmol), BOC-anhydride (48.6
44
45 g, 223 mmol), in EtOH (300 mL) was added 20% $\text{Pd}(\text{OH})_2/\text{C}$ (7.82 g, 50% wet) and the reaction
46
47 was heated at reflux for 1 h. The mixture was then filtered through a Celite® pad and the
48
49 filtrate was concentrated. The residue was purified via FCC (0-5% MeOH/DCM) to give (S)-
50
51 *tert*-butyl 6-methyl-4-oxo-3,4,5,6-tetrahydropyrido[3,4-d]pyrimidine-7(8H)-carboxylate (15.7g,
52
53 80%). MS (ESI) m/z 266.1 (M+H); ^1H NMR (400 MHz, chloroform-d) δ 12.70 (s, 1H), 8.09 (s,
54
55
56
57
58
59
60

1
2
3 1H), 4.85 – 4.65 (m, 2H), 4.03 (d, $J = 19.8$ Hz, 1H), 2.70 (dd, $J = 17.2, 6.0$ Hz, 1H), 2.59 (d, $J =$
4
5 17.2 Hz, 1H), 1.49 (s, 9H), 1.10 (d, $J = 6.9$ Hz, 3H).
6
7

8 A solution of (*S*)-*tert*-butyl 6-methyl-4-oxo-3,4,5,6-tetrahydropyrido[3,4-*d*]pyrimidine-7(8*H*)-
9
10 carboxylate, (15.1 g, 57.1 mmol), triphenylphosphine (29.9 g, 114 mmol) and carbon
11
12 tetrachloride (16.5 mL, 171 mmol) in 1,2-DCE (300 mL) was heated at 70 °C for 3 h. At that
13
14 time the solution was concentrated in vacuo and the residue was separated via FCC (5-60%
15
16 EtOAc/heptane) to give (*S*)-*tert*-Butyl 4-chloro-6-methyl-5,6-dihydropyrido[3,4-*d*]pyrimidine-
17
18 7(8*H*)-carboxylate (**21**) (8.22 g, 51%). MS (ESI) m/z 284.1 (M+H). ¹H NMR (400 MHz,
19
20 chloroform-*d*) δ 8.78 (s, 1H), 4.96 (d, $J = 19.7$ Hz, 1H), 4.84 (s, 1H), 4.25 (d, $J = 19.7$ Hz, 1H),
21
22 2.99 (dd, $J = 17.1, 5.9$ Hz, 1H), 2.74 (d, $J = 17.1$ Hz, 1H), 1.48 (s, 9H), 1.11 (d, $J = 7.0$ Hz, 3H).
23
24
25
26

27 **(*R*)-*tert*-Butyl 4-chloro-6-methyl-5,6-dihydropyrido[3,4-*d*]pyrimidine-7(8*H*)-carboxylate**
28
29 (**22**). Prepared as described for **21**. MS (ESI) m/z 284.0 (M+H); ¹H NMR (400 MHz,
30
31 chloroform-*d*) δ 8.81 (s, 1 H) 4.99 (d, $J=19.70$ Hz, 1 H) 4.86 (br. s., 1 H) 4.27 (d, $J=19.96$ Hz, 1
32
33 H) 3.01 (dd, $J=17.18, 6.06$ Hz, 1 H) 2.76 (d, $J=17.18$ Hz, 1 H) 1.41 - 1.56 (m, 9 H) 1.13 (d,
34
35 $J=6.82$ Hz, 3 H).
36
37
38
39
40

41 **4-Oxo-3,4,5,7-tetrahydro-pyrrolo[3,4-*d*]pyrimidine-6-carboxylic acid *tert*-butyl ester**
42
43 (**24**). To a solution of 4-oxo-pyrrolidine-1,3-dicarboxylic acid 1-*tert*-butyl ester 3-ethyl ester (46
44
45 g, 179 mmol) in EtOH (1.5 L), formamidine hydrochloride (112 g, 1073 mmol) was added,
46
47 followed by NaOEt (203 g, 626 mmol). The reaction was heated at 90 °C for 2 h. The reaction
48
49 mixture was then evaporated and a saturated solution of ammonium chloride (300 mL) was
50
51 added followed by DCM (1L). The layers were separated and the aqueous layer was extracted
52
53 further with DCM. The organics were combined, dried and evaporated to give the crude product.
54
55
56
57
58
59
60

1
2
3 The title compound was purified using silica gel FCC (gradient elution 100% DCM to 94%
4 DCM/ 6 % MeOH) (10 g, 24 % yield). ¹H NMR (400 MHz, methanol-d) δ 8.18 (s, 1 H) 4.47 -
5 4.54 (m, 4 H) 1.45 - 1.56 (m, 8 H) 1.41 (s, 1 H) MS (ESI) *m/z* 238.2 (M+1).
6
7
8
9
10

11
12 **5-Methyl-4-oxo-3,4,5,7-tetrahydro-pyrrolo[3,4-*d*]pyrimidine-6-carboxylic acid *tert*-butyl**
13 **ester (28).** To a suspension of NaH (9.72 g, 243 mmol, 60% in mineral oil) in toluene (100 mL),
14 ethyl 2-(*tert*-butoxycarbonylamino)acetate (38 g, 187 mmol) was added at 0 °C. The reaction
15 was stirred for 5 h at the same temperature. At that point ethyl but-2-enoate (25.6 g, 224 mmol)
16 was added and the reaction allowed to warm up to rt and stirred for further 2 h. Ethanol (30 mL)
17 was added and the reaction was then evaporated. The crude 1-*tert*-butyl 3-ethyl 2-methyl-4-
18 oxopyrrolidine-1,3-dicarboxylate was dissolved in EtOH (1500 mL), then formamidine acetate
19 (343 g, 119 mmol) was added followed by sodium ethoxide (47.2 g, 694 mmol). The reaction
20 was left stirring at 90 °C for 8h. The solvent was then removed and to the crude material a
21 saturated solution of NH₄Cl (200 mL) was added followed by DCM (1 L). The water layer was
22 extracted two times with DCM. The organics were dried and evaporated. The crude product was
23 separated by FCC (DCM/MeOH 100:0 to 90:10) to give the title compound (10 g, 21%). MS
24 (ESI) *m/z* 252.2 (M+1); ¹H NMR (400 MHz, MeOD) δ 8.17 (s, 1 H) 4.85 – 4.92 (m, 1 H) 4.40 -
25 4.52 (m, 1 H) 4.02 - 4.19 (m, 1 H) 1.49 - 1.51 (m, 12 H).
26
27
28
29
30
31
32
33
34
35
36
37
38
39
40
41
42
43
44
45
46

47 **4-(1*H*-Indol-5-yloxy)-5,7-dihydro-pyrrolo[3,4-*d*]pyrimidine-6-carboxylic acid *tert*-butyl**
48 **ester (30a).** To a solution of 4-oxo-3,4,5,7-tetrahydro-pyrrolo[3,4-*d*]pyrimidine-6-carboxylic
49 acid *tert*-butyl ester (74 mg, 0.31 mmol) in acetonitrile (3 mL), BOP (179 mg, 0.405 mmol) was
50 added followed by DBU (0.094 mL, 0.624 mmol). After 20 min 5-hydroxyindole (83 mg, 0.624
51 mmol) was added. The reaction was left stirring at rt for 3 h. The reaction mixture was
52
53
54
55
56
57
58
59
60

1
2
3 evaporated and the crude product was purified using silica gel FCC (gradient elution 100%
4 heptane to 60% heptane/40% ethyl acetate) to give the title compound **30a** (70 mg, 64 % yield).
5
6
7
8 ^1H NMR (400 MHz, DMSO- d_6) δ 11.22 (br. s., 1 H) 8.62 (d, $J=4.04$ Hz, 1 H) 7.41 - 7.44 (m, 2
9 H) 7.35 (d, $J=2.27$ Hz, 1 H) 6.92 (d, $J=8.84$ Hz, 1 H) 6.44 (t, $J=2.15$ Hz, 1 H) 4.56 - 4.61 (m, 3 H)
10
11 4.51 (br. s., 1 H) 1.44 - 1.51 (m, 9 H) MS (ESI) m/z 353.1 (M+1).
12
13
14
15

16
17 **(S)-4-(1H-Indol-5-yloxy)-6-methyl-5,8-dihydro-6H-pyrido[3,4-d]pyrimidine-7-carboxylic**
18 **acid tert-butyl ester (30b)**. DBU (2.34 mL, 15.5 mmol) was added to a solution of 5-
19 hydroxyindole (2.17 g, 16.3 mmol), and (S)-tert-Butyl 4-chloro-6-methyl-5,6-dihydropyrido[3,4-
20 d]pyrimidine-7(8H)-carboxylate (**21**) (2.20 g, 7.75 mmol) in acetonitrile (50 mL) under an argon
21 atmosphere. The reaction was heated at 80 °C for 2.5 h. At that time the solution was allowed
22 to cool to rt and the excess solvent was evaporated. The residue was then separated via flash
23 chromatography (30-100% EtOAc) to give the title compound **30b** (2.66 g, 90%). MS (ESI) m/z
24 381.3 (M+1); ^1H NMR (400 MHz, chloroform- d) δ 8.53 (s, 1H), 8.22 (s, 1H), 7.43 (d, $J=8.7$
25 Hz, 1H), 7.39 (d, $J=2.2$ Hz, 1H), 6.97 (dd, $J=8.7, 2.3$ Hz, 1H), 6.56 (t, $J=2.3$ Hz, 1H), 4.95
26 (d, $J=18.5$ Hz, 1H), 4.91 – 4.82 (m, 1H), 4.24 (d, $J=19.1$ Hz, 1H), 3.02 (dd, $J=16.9, 6.4$ Hz,
27 1H), 2.85 (d, $J=16.9$ Hz, 1H), 1.51 (s, 9H), 1.20 (d, $J=6.9$ Hz, 3H).
28
29
30
31
32
33
34
35
36
37
38
39
40
41
42

43 **3-(1-Methyl-cyclopropyl)-5-phenoxy-carbonylamino-pyrazole-1-carboxylic acid tert-butyl**
44 **ester (32a)**. To a solution of 5-amino-3-(1-methyl-cyclopropyl)-pyrazole-1-carboxylic acid *tert*-
45 butyl ester²⁹ (3.90 g, 16.4 mmol) and phenyl chloroformate (3.11 mL, 24.6 mmol) in DCM (150
46 mL) was added 2,6-lutidine (5.74 mL, 49.3 mmol). After 18 h the solution was diluted with
47 DCM (100 mL) and washed with 1 M HCl (250 mL). The organic layer was then dried
48 (Na₂SO₄), filtered, and concentrated to provide the title compound (5.07 g, 86% yield). MS (ESI)
49
50
51
52
53
54
55
56
57
58
59
60

1
2
3 m/z 358.0 (M+1); ^1H NMR (400 MHz, dichloromethane- d_2) δ 9.76 (br. s., 1 H) 7.38 - 7.45 (m, 2
4
5 H) 7.24 - 7.30 (m, 1 H) 7.16 - 7.22 (m, 2 H) 6.33 (s, 1 H) 1.57 - 1.74 (m, 9 H) 1.42 (s, 3 H) 0.89 -
6
7
8 1.06 (m, 2 H) 0.56 - 0.84 (m, 2 H).
9

10
11
12 **5-((S)-6-Methyl-5,6,7,8-tetrahydro-pyrido[3,4-*d*]pyrimidin-4-yloxy)-indole-1-carboxylic**
13 **acid [5-(1-methyl-cyclopropyl)-2*H*-pyrazol-3-yl]-amide (33n).** Sodium hydride (2.27 g, 56.8
14
15 mmol; 60% in oil) was added to a solution of (*S*)-4-(1*H*-indol-5-yloxy)-6-methyl-5,8-*d*ihydro-
16
17 6*H*-pyrido[3,4-*d*]pyrimidine-7-carboxylic acid *tert*-butyl ester (7.20 g, 18.9 mmol) and 3-(1-
18
19 methyl-cyclopropyl)-5-phenoxy-carbonylamino-pyrazole-1-carboxylic acid *tert*-butyl ester (8.12
20
21 g, 22.7 mmol) in THF (250 mL) at 0 °C under argon. After 2 h the reaction was quenched by
22
23 slow addition to a stirred solution of saturated aqueous NH_4Cl (1 L) the resulting slurry was then
24
25 extracted with DCM (3 x 700 mL) and the combined organic layers were dried over sodium
26
27 sulfate, filtered and concentrated. The residue was separated directly via FCC (20-50%
28
29 EtOAc/heptane) to give (*S*)-4-{1-[2-*tert*-butoxycarbonyl-5-(1-methyl-cyclopropyl)-2*H*-pyrazol-
30
31 3-ylcarbamoyl]-1*H*-indol-5-yloxy}-6-methyl-5,8-*d*ihydro-6*H*-pyrido[3,4-*d*]pyrimidine-7-
32
33 carboxylic acid *tert*-butyl ester (6.10 g, 50%). MS (ESI) m/z 644.2 (M+1); ^1H NMR (400 MHz,
34
35 DMSO- d_6) δ 10.38 (s, 1H), 8.50 (s, 1H), 8.26 (d, $J = 9.0$ Hz, 1H), 7.92 (d, $J = 3.7$ Hz, 1H), 7.49
36
37 (d, $J = 2.4$ Hz, 1H), 7.16 (dd, $J = 8.9, 2.4$ Hz, 1H), 6.82 (d, $J = 3.7$ Hz, 1H), 6.37 (s, 1H), 4.79 -
38
39 4.66 (m, 2H), 4.22 (d, $J = 20.4$ Hz, 1H), 2.95 (dd, $J = 17.1, 6.7$ Hz, 1H), 2.79 (d, $J = 16.8$ Hz,
40
41 1H), 1.46 (s, 9H), 1.45 (s, 9H), 1.41 (s, 3H), 1.12 (d, $J = 6.9$ Hz, 3H), 0.96 (q, $J = 4.0$ Hz, 2H),
42
43 0.82 - 0.77 (m, 2H).
44
45
46
47
48
49
50
51
52

53 A solution of (*S*)-4-{1-[2-*tert*-Butoxycarbonyl-5-(1-methyl-cyclopropyl)-2*H*-pyrazol-3-
54
55 ylcarbamoyl]-1*H*-indol-5-yloxy}-6-methyl-5,8-*d*ihydro-6*H*-pyrido[3,4-*d*]pyrimidine-7-
56
57
58
59
60

1
2
3 carboxylic acid *tert*-butyl ester (6.10 g, 9.48 mmol) in DCM (50 mL) was cooled to 0 °C, and
4
5 TFA (15 mL) was added slowly. After 20 min the ice bath was removed and the contents
6
7 allowed to reach room temperature. After 2 h at that temperature the solvent was removed under
8
9 reduced pressure. The residue was taken up in water (250 mL) and acetonitrile (25 mL) and
10
11 stirred. Aqueous NH₄OH (28%) was then added until pH 9. The slurry was stirred for 15 min
12
13 before the solid was collected filtration. The solid was slurried a second time in dilute aqueous
14
15 NH₄OH and the solid collected by filtration. The solid was then dried to give the title compound
16
17 **33n** (3.87 g, 92%). MS (ESI) *m/z* 444.1 (M+1); ¹H NMR (400 MHz, DMSO-*d*₆) δ 12.13 (br. S.,
18
19 1 H), 10.55 (s, 1 H), 8.40 (s, 1 H), 8.29 (d, *J*=8.8 Hz, 1 H), 8.16 (d, *J*=3.5 Hz, 1 H), 7.40 (d,
20
21 *J*=2.3 Hz, 1 H), 7.08 (dd, *J*=9.1, 2.3 Hz, 1 H), 6.70 (d, *J*=3.8 Hz, 1 H), 6.30 (s, 1 H), 3.76 – 3.98
22
23 (m, 2 H), 2.92 – 3.05 (m, 1 H), 2.85 (dd, *J*=16.5, 3.4 Hz, 1 H), 2.27 – 2.40 (m, 1 H), 1.41 (s, 3
24
25 H), 1.22 (d, *J*=6.3 Hz, 3 H), 0.89 – 0.97 (m, 2 H), 0.73 – 0.82 (m, 2 H).
26
27
28
29
30
31
32
33

34 **5-(6-Hydroxymethyl-pyrimidin-4-yloxy)-indole-1-carboxylic acid (3-trifluoromethyl-**
35
36 **phenyl)-amide (5a)**. MS (ESI) *m/z* 429.1 (M+1); ¹H NMR (400 MHz, methanol-*d*₄) δ 8.61 (d,
37
38 *J*=1.01 Hz, 1 H), 8.37 (d, *J*=8.84 Hz, 1 H), 8.07 (s, 1 H), 7.96 (d, *J*=3.79 Hz, 1 H), 7.90 (dd,
39
40 *J*=7.96, 1.39 Hz, 1 H), 7.58 (t, *J*=7.96 Hz, 1 H), 7.45 (s, 1 H), 7.43 (d, *J*=2.27 Hz, 1 H), 7.13 (dd,
41
42 *J*=8.97, 2.40 Hz, 1 H), 7.08 (d, *J*=1.01 Hz, 1 H), 6.76 (d, *J*=3.79 Hz, 1 H), 4.63 (s, 2 H).
43
44
45
46
47

48 **5-((6-((methylamino)methyl)pyrimidin-4-yl)oxy)-N-(3-(trifluoromethyl)phenyl)-1H-**
49
50 **indole-1-carboxamide (6a)**. MS (ESI) *m/z* 442.1 (M+1); ¹H NMR (400 MHz, methanol-*d*₄) δ
51
52 8.64 (s, 1 H), 8.34 (d, *J*=9.09 Hz, 1 H), 8.05 (s, 1 H), 7.93 (d, *J*=3.79 Hz, 1 H), 7.89 (d, *J*=8.08
53
54
55
56
57
58
59
60

1
2
3 Hz, 1 H), 7.56 (t, $J=7.96$ Hz, 1 H), 7.40 – 7.46 (m, 2 H), 7.10 (dd, $J=8.97$, 2.40 Hz, 1 H), 6.99 (s,
4
5
6 1 H), 6.73 (d, $J=3.79$ Hz, 1 H), 3.77 (s, 2 H), 2.40 (s, 3 H).
7
8
9

10 **N-(4-fluoro-3-(trifluoromethyl)phenyl)-5-((6-((methylamino)methyl)pyrimidin-4-yl)oxy)-**
11
12 **1H-indole-1-carboxamide (6b)**. MS (ESI) m/z 460.1 (M+1); ^1H NMR (400 MHz, methanol- d_4)
13
14 δ 8.65 (d, $J=1.01$ Hz, 1 H), 8.35 (d, $J=8.84$ Hz, 1 H), 8.04 (dd, $J=6.19$, 2.65 Hz, 1 H), 7.90 – 7.94
15
16 (m, 2 H), 7.41 (d, $J=2.27$ Hz, 1 H), 7.35 (t, $J=9.60$ Hz, 1 H), 7.11 (dd, $J=8.97$, 2.40 Hz, 1 H),
17
18 7.00 (s, 1 H), 6.74 (d, $J=3.79$ Hz, 1 H), 3.82 (s, 2 H), 2.43 (s, 3 H).
19
20
21
22
23

24 **5-((5,6,7,8-tetrahydropyrido[3,4-d]pyrimidin-4-yl)oxy)-N-(3-(trifluoromethyl)phenyl)-1H-**
25
26 **indole-1-carboxamide (33a)**. MS (ESI) m/z 454.0 (M+1); ^1H NMR (400 MHz, DMSO- d_6) δ
27
28 10.43 (s, 1 H), 8.54 (s, 1 H), 8.30 (d, $J=8.8$ Hz, 1 H), 8.15 (d, $J=3.5$ Hz, 1 H), 8.11 (s, 1 H), 7.98
29
30 (d, $J=8.3$ Hz, 1 H), 7.65 (t, $J=8.0$ Hz, 1 H), 7.44 – 7.53 (m, 2 H), 7.14 (dd, $J=9.0$, 2.4 Hz, 1 H),
31
32 6.81 (d, $J=3.8$ Hz, 1 H), 4.26 (s, 2 H), 3.45 (t, $J=5.9$ Hz, 2 H), 3.00 (t, $J=5.8$ Hz, 2 H).
33
34
35
36
37
38

39 **5-((5,6,7,8-tetrahydropyrido[4,3-d]pyrimidin-4-yl)oxy)-N-(3-(trifluoromethyl)phenyl)-1H-**
40
41 **indole-1-carboxamide (33b)**. MS (ESI) m/z 454.0 (M+1); ^1H NMR (400 MHz, DMSO- d_6) δ
42
43 10.38 (s, 1 H), 8.46 (s, 1 H), 8.27 (d, $J=9.1$ Hz, 1 H), 8.12 (d, $J=3.8$ Hz, 1 H), 8.10 (s, 1 H), 7.97
44
45 (d, $J=8.1$ Hz, 1 H), 7.65 (t, $J=8.0$ Hz, 1 H), 7.50 (d, $J=7.3$ Hz, 1 H), 7.46 (s, 1 H), 7.12 (dd,
46
47 $J=9.0$, 2.4 Hz, 1 H), 6.80 (d, $J=3.5$ Hz, 1 H), 3.92 – 4.09 (m, 2 H), 3.17 (t, $J=5.7$ Hz, 2 H), 2.81
48
49 (t, $J=5.7$ Hz, 2 H).
50
51
52
53
54
55
56
57
58
59
60

1
2
3
4
5
6
7
8
9
10
11
12
13
14
15
16
17
18
19
20
21
22
23
24
25
26
27
28
29
30
31
32
33
34
35
36
37
38
39
40
41
42
43
44
45
46
47
48
49
50
51
52
53
54
55
56
57
58
59
60

(S)-5-((6-methyl-5,6,7,8-tetrahydropyrido[3,4-d]pyrimidin-4-yl)oxy)-N-(3-(trifluoromethyl)phenyl)-1H-indole-1-carboxamide (33c). MS (ESI) m/z 468.2 (M+1); ^1H NMR (400 MHz, methanol- d_4) δ 8.37 (s, 1 H) 8.32 (d, $J=8.84$ Hz, 1 H) 8.05 (s, 1 H) 7.92 (d, $J=3.79$ Hz, 1 H) 7.89 (d, $J=8.59$ Hz, 1 H) 7.56 (t, $J=7.96$ Hz, 1 H) 7.44 (d, $J=7.83$ Hz, 1 H) 7.39 (d, $J=2.27$ Hz, 1 H) 7.09 (dd, $J=8.97, 2.40$ Hz, 1 H) 6.73 (d, $J=3.79$ Hz, 1 H) 3.89 – 4.09 (m, 2 H) 3.05 – 3.16 (m, 1 H) 2.99 (dd, $J=17.18, 3.79$ Hz, 1 H) 2.47 (dd, $J=17.18, 10.36$ Hz, 1 H) 1.34 (d, $J=6.57$ Hz, 3 H).

(R)-5-((6-methyl-5,6,7,8-tetrahydropyrido[3,4-d]pyrimidin-4-yl)oxy)-N-(3-(trifluoromethyl)phenyl)-1H-indole-1-carboxamide (33d). MS (ESI) m/z 468.2 (M+1); ^1H NMR (400 MHz, methanol- d_4) δ 8.37 (s, 1 H) 8.32 (d, $J=8.84$ Hz, 1 H) 8.05 (s, 1 H) 7.92 (d, $J=3.79$ Hz, 1 H) 7.89 (d, $J=8.59$ Hz, 1 H) 7.56 (t, $J=7.96$ Hz, 1 H) 7.44 (d, $J=7.83$ Hz, 1 H) 7.39 (d, $J=2.27$ Hz, 1 H) 7.09 (dd, $J=8.97, 2.40$ Hz, 1 H) 6.73 (d, $J=3.79$ Hz, 1 H) 3.89 – 4.09 (m, 2 H) 3.05 – 3.16 (m, 1 H) 2.99 (dd, $J=17.18, 3.79$ Hz, 1 H) 2.47 (dd, $J=17.18, 10.36$ Hz, 1 H) 1.34 (d, $J=6.57$ Hz, 3 H).

5-((7-acetyl-5,6,7,8-tetrahydropyrido[3,4-d]pyrimidin-4-yl)oxy)-N-(3-(trifluoromethyl)phenyl)-1H-indole-1-carboxamide (33e). MS (ESI) m/z 496.0 (M+1); ^1H NMR (400 MHz, DMSO- d_6) δ 10.38 (s, 1 H), 8.45 – 8.53 (m, 1 H), 8.27 (d, $J=9.1$ Hz, 1 H), 8.12 (d, $J=3.8$ Hz, 1 H), 8.10 (s, 1 H), 7.97 (d, $J=8.8$ Hz, 1 H), 7.65 (t, $J=8.1$ Hz, 1 H), 7.50 (d, $J=7.8$ Hz, 1 H), 7.47 (d, $J=2.3$ Hz, 1 H), 7.14 (dd, $J=9.0, 2.4$ Hz, 1 H), 6.80 (d, $J=3.5$ Hz, 1 H), 4.63 (s, 2 H), 3.81 (t, $J=5.9$ Hz, 2 H), 2.93 (t, $J=5.7$ Hz, 2 H), 2.16 (s, 3 H).

1
2
3
4
5
6
7
8
9
10
11
12
13
14
15
16
17
18
19
20
21
22
23
24
25
26
27
28
29
30
31
32
33
34
35
36
37
38
39
40
41
42
43
44
45
46
47
48
49
50
51
52
53
54
55
56
57
58
59
60

5-((7-ethyl-5,6,7,8-tetrahydropyrido[3,4-d]pyrimidin-4-yl)oxy)-N-(3-(trifluoromethyl)phenyl)-1H-indole-1-carboxamide (33f). MS (ESI) m/z 482.2 (M+1); ^1H NMR (400 MHz, DMSO- d_6) δ 10.38 (br. S., 1 H), 8.42 (s, 1 H), 8.28 (d, $J=9.1$ Hz, 1 H), 8.11 (d, $J=3.8$ Hz, 1 H), 8.10 (s, 1 H), 7.96 (d, $J=9.1$ Hz, 1 H), 7.63 (t, $J=8.0$ Hz, 1 H), 7.48 (d, $J=7.8$ Hz, 1 H), 7.46 (d, $J=2.5$ Hz, 1 H), 7.13 (dd, $J=9.0, 2.4$ Hz, 1 H), 6.78 (d, $J=3.8$ Hz, 1 H), 3.57 (s, 2 H), 2.74 – 2.87 (m, 4 H), 2.59 (q, $J=7.2$ Hz, 2 H), 1.12 (t, $J=7.2$ Hz, 3 H).

5-((6,7-dihydro-5H-pyrrolo[3,4-d]pyrimidin-4-yl)oxy)-N-(3-(trifluoromethyl)phenyl)-1H-indole-1-carboxamide (33g). MS (ESI) m/z 440.9 (M+1); ^1H NMR (400 MHz, methanol- d_4) δ 8.55 (s, 1 H) 8.33 (d, $J=8.84$ Hz, 1 H) 8.06 (br. S., 1 H) 7.89 (d, $J=8.34$ Hz, 1 H) 7.94 (d, $J=3.54$ Hz, 1 H) 7.57 (t, $J=7.96$ Hz, 1 H) 7.41 – 7.46 (m, 2 H) 7.13 (dd, $J=9.09, 2.27$ Hz, 1 H) 6.74 (d, $J=3.03$ Hz, 1 H) 4.26 (d, $J=12.13$ Hz, 4 H).

(S)-5-(5-Methyl-6,7-dihydro-5H-pyrrolo[3,4-d]pyrimidin-4-yloxy)-indole-1-carboxylic acid (3-trifluoromethyl-phenyl)-amide (33h). MS (ESI) m/z 454.9 (M+1); ^1H NMR (400 MHz, methanol- d_4) δ 8.47 (d, $J=1.77$ Hz, 1 H) 8.28 (dd, $J=9.09, 1.77$ Hz, 1 H) 8.02 (s, 1 H) 7.85 (dd, $J=3.66, 2.40$ Hz, 2 H) 7.49 (t, $J=7.83$ Hz, 1 H) 7.36 (d, $J=2.02$ Hz, 1 H) 7.38 (d, $J=8.59$ Hz, 1 H) 7.06 (dd, $J=8.84, 2.27$ Hz, 1 H) 6.65 (d, $J=2.53$ Hz, 1 H) 4.63 (d, $J=6.06$ Hz, 1 H) 4.15 – 4.23 (m, 1 H) 4.05 – 4.12 (m, 1 H) 1.55 (d, $J=6.57$ Hz, 3 H).

1
2
3
4 **(R)-5-(5-Methyl-6,7-dihydro-5H-pyrrolo[3,4-d]pyrimidin-4-yloxy)-indole-1-carboxylic**
5
6 **acid (3-trifluoromethyl-phenyl)-amide (33i).** MS (ESI) m/z 454.9 (M+1); ^1H NMR (400 MHz,
7
8 methanol- d_4) δ 8.48 (s, 1 H) 8.30 (d, $J=9.09$ Hz, 1 H) 8.03 (s, 1 H) 7.87 (d, $J=3.54$ Hz, 2 H) 7.52
9
10 (t, $J=8.08$ Hz, 1 H) 7.38 (d, $J=2.27$ Hz, 2 H) 7.07 (dd, $J=8.84, 2.27$ Hz, 1 H) 6.67 (d, $J=3.79$ Hz,
11
12 1 H) 4.66 (q, $J=6.57$ Hz, 1 H) 4.12-4.22 (m, 2 H) 1.56 (d, $J=6.57$ Hz, 3 H).
13
14
15
16
17
18
19

20 **5-(5,6,7,8-Tetrahydro-pyrido[3,4-d]pyrimidin-4-yloxy)-indole-1-carboxylic acid (5-**
21 **methyl-pyridin-3-yl)-amide (33j).** MS (ESI) m/z 401.1 (M+1); ^1H NMR (methanol- d_4) δ 8.64
22
23 (d, $J=2.0$ Hz, 1 H), 8.37 (s, 1 H), 8.33 (d, $J=8.8$ Hz, 1 H), 8.18 (d, $J=1.0$ Hz, 1 H), 8.03 (s, 1 H),
24
25 7.92 (d, $J=3.5$ Hz, 1 H), 7.40 (d, $J=2.3$ Hz, 1 H), 7.10 (dd, $J=9.1, 2.3$ Hz, 1 H), 6.74 (d, $J=3.0$ Hz,
26
27 1 H), 3.95 (s, 2 H), 3.18 (t, $J=5.9$ Hz, 2 H), 2.88 (t, $J=5.8$ Hz, 2 H), 2.41 (s, 3 H).
28
29
30
31
32
33
34
35
36
37

38 **5-(5,6,7,8-Tetrahydro-pyrido[3,4-d]pyrimidin-4-yloxy)-indole-1-carboxylic acid (5-**
39 **isopropyl-1H-pyrazol-3-yl)-amide (33k).** MS (ESI) m/z 418.2 (M+1); ^1H NMR (DMSO- d_6) δ
40
41 12.21 (br. S., 1 H), 10.56 (s, 1 H), 8.39 (s, 1 H), 8.29 (d, $J=9.1$ Hz, 1 H), 8.16 (d, $J=3.5$ Hz, 1 H),
42
43 7.41 (d, $J=2.3$ Hz, 1 H), 7.08 (dd, $J=9.1, 2.3$ Hz, 1 H), 6.70 (d, $J=3.5$ Hz, 1 H), 6.34 (s, 1 H), 3.81
44
45 (s, 2 H), 2.87 – 3.07 (m, 3 H), 2.72 (t, $J=5.6$ Hz, 2 H), 1.25 (d, $J=6.8$ Hz, 6 H).
46
47
48
49
50
51
52

53 **5-(5,6,7,8-Tetrahydro-pyrido[3,4-d]pyrimidin-4-yloxy)-indole-1-carboxylic acid (5-tert-**
54 **butyl-2H-pyrazol-3-yl)-amide (33l).** MS (ESI) m/z 432.1 (M+1); ^1H NMR (methanol- d_4) δ 8.37
55
56
57
58
59
60

1
2
3 (s, 1 H), 8.32 (d, $J=8.8$ Hz, 1 H), 7.88 (d, $J=3.5$ Hz, 1 H), 7.38 (d, $J=2.3$ Hz, 1 H), 7.08 (dd,
4
5 $J=9.1, 2.3$ Hz, 1 H), 6.71 (d, $J=3.8$ Hz, 1 H), 6.37 (s, 1 H), 3.96 (s, 2 H), 3.19 (t, $J=5.9$ Hz, 2 H),
6
7
8 2.89 (t, $J=5.7$ Hz, 2 H), 1.36 (s, 9 H).
9

10
11
12
13
14
15 **5-(5,6,7,8-Tetrahydro-pyrido[3,4-*d*]pyrimidin-4-yloxy)-indole-1-carboxylic acid [5-(1-**
16
17 **methyl-cyclopropyl)-2*H*-pyrazol-3-yl]-amide (33m).** HRMS (ESI+) m/z calculated for

18
19 $C_{23}H_{23}N_7O_2$ (M+1) 430.1993, found 430.1992; 1H NMR (DMSO- d_6) δ 12.13 (br. S., 1 H), 10.55
20
21 (s, 1 H), 8.40 (s, 1 H), 8.29 (d, $J=8.8$ Hz, 1 H), 8.16 (d, $J=3.8$ Hz, 1 H), 7.41 (d, $J=2.3$ Hz, 1 H),
22
23 7.08 (dd, $J=9.0, 2.4$ Hz, 1 H), 6.70 (d, $J=3.5$ Hz, 1 H), 6.29 (s, 1 H), 3.84 (s, 2 H), 3.05 (t, $J=5.8$
24
25 Hz, 2 H), 2.69 – 2.78 (m, 2 H), 1.41 (s, 3 H), 1.25 (br. S., 2 H), 0.89 – 0.97 (m, 2 H); ^{13}C NMR
26
27 (400 MHz, DMSO- d_6) δ 166.9, 165.7, 154.3, 149.1, 148.7, 147.5, 146.5, 132.9, 130.2, 126.4,
28
29 118.0, 115.7, 115.4, 113.2, 106.2, 93.8, 49.4, 41.9, 22.6, 22.0, 15.6, 12.6.
30
31
32
33

34
35 **5-((*S*)-6-Methyl-5,6,7,8-tetrahydro-pyrido[3,4-*d*]pyrimidin-4-yloxy)-indole-1-carboxylic**
36
37 **acid [5-(1-methyl-cyclopropyl)-2*H*-pyrazol-3-yl]-amide (33n).** HRMS (ESI+) m/z calculated
38
39 for $C_{24}H_{25}N_7O_2$ (M+1) 444.2149, found 444.2143; 1H NMR (400 MHz, DMSO- d_6) δ 12.13 (br.
40
41 S., 1 H), 10.55 (s, 1 H), 8.40 (s, 1 H), 8.29 (d, $J=8.8$ Hz, 1 H), 8.16 (d, $J=3.5$ Hz, 1 H), 7.40 (d,
42
43 $J=2.3$ Hz, 1 H), 7.08 (dd, $J=9.1, 2.3$ Hz, 1 H), 6.70 (d, $J=3.8$ Hz, 1 H), 6.30 (s, 1 H), 3.76 – 3.98
44
45 (m, 2 H), 2.92 – 3.05 (m, 1 H), 2.85 (dd, $J=16.5, 3.4$ Hz, 1 H), 2.27 – 2.40 (m, 1 H), 1.41 (s, 3
46
47 H), 1.22 (d, $J=6.3$ Hz, 3 H), 0.89 – 0.97 (m, 2 H), 0.73 – 0.82 (m, 2 H); ^{13}C NMR (400 MHz,
48
49 DMSO- d_6) δ 166.8, 165.1, 154.4, 149.1, 148.7, 147.5, 146.5, 132.9, 130.2, 126.4, 118.0, 115.7,
50
51 115.1, 113.2, 106.3, 93.8, 49.4, 47.7, 29.6, 22.6, 21.5, 15.6, 12.6.
52
53
54
55
56
57
58
59
60

1
2
3
4
5
6
7
8
9
10
11
12
13
14
15
16
17
18
19
20
21
22
23
24
25
26
27
28
29
30
31
32
33
34
35
36
37
38
39
40
41
42
43
44
45
46
47
48
49
50
51
52
53
54
55
56
57
58
59
60

5-(6,7-dihydro-5H-pyrrolo[3,4-d]pyrimidin-4-yloxy)-indole-1-carboxylic acid [5-(1-methyl-cyclopropyl)-2H-pyrazol-3-yl]-amide (33o). MS (ESI) m/z 416.2 (M+1); ^1H NMR (400 MHz, DMSO- d_6) δ 12.13 (s, 1H) 10.57 (s, 1 H) 8.55 (s, 1 H) 8.29 (d, $J=9.09$ Hz, 1 H) 8.17 (d, $J=3.79$ Hz, 1 H) 7.44 (d, $J=2.27$ Hz, 1 H) 7.11 (dd, $J=9.09, 2.53$ Hz, 1 H) 6.71 (d, $J=3.54$ Hz, 1 H) 6.29 (s, 1 H) 4.09 (d, $J=12.63$ Hz, 4 H) 1.41 (s, 3 H) 0.91-0.93 (m, 2 H) 0.74-0.78 (m, 2 H).

5-(R)-6-Methyl-5,6,7,8-tetrahydro-pyrido[3,4-d]pyrimidin-4-yloxy)-indole-1-carboxylic acid [5-(1-methyl-cyclopropyl)-2H-pyrazol-3-yl]-amide (33p). MS (ESI) m/z 444.1 (M+1); ^1H NMR (400 MHz, methanol- d_4) δ 8.51 (s, 1 H), 8.34 (d, $J=9.0$ Hz, 1 H), 7.90 (d, $J=3.8$ Hz, 1 H), 7.41 (d, $J=2.1$ Hz, 1 H), 7.10 (dd, $J=9.0, 2.3$ Hz, 1 H), 6.72 (d, $J=3.7$ Hz, 1 H), 6.28 (s, 1 H), 3.73 – 3.88 (m, 1 H), 2.86 (dd, $J=17.9, 10.7$ Hz, 1 H), 1.59 (d, $J=6.4$ Hz, 3 H), 1.46 (s, 3 H), 0.92 – 1.03 (m, 2 H), 0.75 – 0.88 (m, 2 H).

5-(5,6,7,8-Tetrahydro-pyrido[3,4-d]pyrimidin-4-yloxy)-indole-1-carboxylic acid (5-tert-butyl-isoxazol-3-yl)-amide (33q). MS (ESI) m/z 432.9 (M+1); ^1H NMR (400 MHz, methanol- d_4) δ 8.37 (s, 1 H) 8.33 (d, $J=8.84$ Hz, 1 H) 7.88 (d, $J=3.79$ Hz, 1 H) 7.38 (d, $J=2.02$ Hz, 1 H) 7.10 (dd, $J=8.84, 2.27$ Hz, 1 H) 6.72 (d, $J=3.79$ Hz, 1 H) 6.65 (s, 1 H) 3.94 (s, 2 H) 3.17 (t, $J=5.94$ Hz, 2 H) 2.87 (t, $J=5.68$ Hz, 2 H) 1.38 (s, 9 H).

5-((S)-6-Methyl-5,6,7,8-tetrahydro-pyrido[3,4-d]pyrimidin-4-yloxy)-indole-1-carboxylic acid (5-tert-butyl-isoxazol-3-yl)-amide (33r). MS (ESI) m/z 447.2 (M+1); ^1H NMR (400 MHz, DMSO- d_6) δ 8.40 (s, 1 H) 8.29 (d, $J=9.09$ Hz, 1 H) 8.15 (d, $J=3.28$ Hz, 1 H) 7.43 (d, $J=1.26$ Hz, 1 H) 7.11 (dd, $J=8.72, 1.39$ Hz, 1 H) 6.75 (d, $J=3.03$ Hz, 1 H) 6.68 (s, 1 H) 3.79 – 3.98 (m, 2 H) 2.91 – 3.05 (m, 1 H) 2.85 (d, $J=16.17$ Hz, 1 H) 2.34 (dd, $J=16.17, 9.60$ Hz, 1 H) 1.34 (s, 9 H) 1.21 (d, $J=6.32$ Hz, 3 H).

1
2
3
4 **5-(6,7-dihydro-5H-pyrrolo[3,4-d]pyrimidin-4-yloxy)-indole-1-carboxylic acid (5-tert-butyl-**
5 **isoxazol-3-yl)-amide (33s).** MS (ESI) m/z 419.2 (M+1); ^1H NMR (400 MHz, DMSO- d_6) δ 8.56
6
7 (s, 1 H) 8.29 (d, $J=8.84$ Hz, 1 H) 8.17 (d, $J=3.79$ Hz, 1 H) 7.47 (d, $J=2.27$ Hz, 1 H) 7.15 (dd,
8
9 $J=8.97$, 2.40 Hz, 1 H) 6.76 (d, $J=3.28$ Hz, 1 H) 6.68 (s, 1 H) 4.07 – 4.14 (m, 4 H) 1.34 (s, 9 H).

10
11
12
13
14 **6,7-dihydro-5H-pyrrolo[3,4-d] pyrimidin-4-yloxy)-indole-1-carboxylic acid (3-tert-butyl-**
15 **isoxazol-5-yl)-amide (33t).** MS (ESI) m/z 419.9 (M+1); ^1H NMR (400 MHz, DMSO- d_6) δ 8.61
16
17 (s, 1 H) 8.42 (d, $J=9.09$ Hz, 1 H) 8.11 (d, $J=3.79$ Hz, 1 H) 7.44 (d, $J=2.27$ Hz, 1 H) 7.11 (dd,
18
19 $J=9.22$, 2.40 Hz, 1 H) 6.67 (d, $J=3.54$ Hz, 1 H) 6.22 (s, 1 H) 4.25 (br. S., 4 H) 1.28 (s, 9 H).

20
21
22
23
24
25
26
27 **(S)- 5-(Methyl-6,7-dihydro-5H-pyrrolo[3,4-d]pyrimidin-4-yloxy)-indole-1-carboxylic acid**
28 **(5-tert-butyl-isoxazol-3-yl)-amide (33u).** MS (ESI) m/z 433.0 (M+1); ^1H NMR (400 MHz,
29
30 DMSO- d_6) δ 8.54 (s, 1 H) 8.30 (d, $J=9.09$ Hz, 1 H) 8.16 (d, $J=3.79$ Hz, 1 H) 7.46 (d, $J=2.27$ Hz,
31
32 1 H) 7.14 (dd, $J=8.97$, 2.40 Hz, 1 H) 6.76 (d, $J=3.79$ Hz, 1 H) 6.68 (s, 1 H) 4.62 (d, $J=6.57$ Hz, 1
33
34 H) 4.12 (d, $J=2.27$ Hz, 1 H) 4.08 (d, $J=1.52$ Hz, 1 H) 1.44 (d, $J=6.57$ Hz, 3 H) 1.34 (s, 9 H).

35
36
37
38
39
40
41 **5-(6,7-dihydro-5H-pyrrolo[3,4-d] pyrimidin-4-yloxy)-indole-1-carboxylic acid (5-**
42 **cyclopropyl-isoxazol-3-yl)-amide (33v).** HRMS (ESI+) m/z calculated for $\text{C}_{21}\text{H}_{18}\text{N}_6\text{O}_3$ (M+1)
43
44 403.1520, found 403.1520; ^1H NMR (400 MHz, DMSO- d_6) δ 8.55 (s, 1 H) 8.29 (d, $J=9.09$ Hz, 1
45
46 H) 8.16 (d, $J=3.79$ Hz, 1 H) 7.46 (d, $J=2.27$ Hz, 1 H) 7.14 (dd, $J=8.97$, 2.40 Hz, 1 H) 6.75 (d,
47
48 $J=3.28$ Hz, 1 H) 6.65 (s, 1 H) 4.04 – 4.16 (m, 4 H) 2.07 – 2.26 (m, 1 H) 1.01 – 1.15 (m, 2 H) 0.87
49
50 – 0.98 (m, 2 H); ^{13}C NMR (400 MHz, DMSO- d_6) δ 175.2, 174.6, 164.4, 158.7, 157.3, 149.1,
51
52 147.7, 133.1, 130.6, 126.7, 118.5, 118.4, 116.0, 113.5, 107.2, 93.9, 52.8, 487.9, 8.2, 8.0.
53
54
55
56
57
58
59
60

1
2
3
4
5
6 **5-(6,7-dihydro-5H-pyrrolo[3,4-d] pyrimidin-4-yloxy)-indole-1-carboxylic acid (5-**
7
8 **isopropyl-isoxazol-3-yl)-amide (33w).** MS (ESI) m/z 405.1 (M+1); ^1H NMR (400 MHz,
9
10 DMSO- d_6) δ 8.56 (s, 1 H) 8.29 (d, $J=8.84$ Hz, 1 H) 8.17 (d, $J=3.79$ Hz, 1H) 7.47 (d, $J=2.27$ Hz, 1
11
12 H) 7.15 (dd, $J=8.97$, 2.40 Hz, 1 H) 6.76 (d, $J=3.79$ Hz, 1 H) 6.69 (s, 1 H) 4.00 – 4.20 (m, 4 H)
13
14 3.11 (m, 1 H) 1.29 (d, $J=7.07$ Hz, 6 H).
15
16
17
18
19

20 **5-(6,7-dihydro-5H-pyrrolo[3,4-d] pyrimidin-4-yloxy)-indole-1-carboxylic acid [5-(1-**
21
22 **methyl-cyclopropyl)-isoxazol-3-yl]-amide (33x).** MS (ESI) m/z 417.1 (M+1); ^1H NMR (400
23
24 MHz, DMSO- d_6) δ 8.56 (s, 1 H) 8.29 (d, $J=8.84$ Hz, 1 H) 8.16 (d, $J=3.79$ Hz, 1 H) 7.47 (d,
25
26 $J=2.53$ Hz, 1 H) 7.15 (dd, $J=8.97$, 2.40 Hz, 1 H) 6.76 (d, $J=3.28$ Hz, 1 H) 6.67 (s, 1 H) 4.01 –
27
28 4.19 (m, 4 H + 1 N-H) 1.46 (s, 3 H) 1.07 – 1.21 (m, 2 H) 0.86 – 1.02 (m, 2 H).
29
30
31
32
33

34 **Mouse Laser-Induced Choroidal Neovascularization (CNV) Model.**

35
36 Animal research presented in this paper was approved by the Novartis Institutes for
37
38 Biomedical Research IACUC Committee. We used female C57/BL6 mice that were typically 8 -
39
40 10 weeks old. Mice used in an experiment arrived at our research facility in a single shipment.
41
42 Experimental interventions for a cohort of animals were started on the same day. Mice were
43
44 treated by oral gavage with compound starting 1 hour before laser (Day 0) and continuing once
45
46 a day through Day 6 after laser. Experimental groups were dosed with either vehicle (0.5%
47
48 methylcellulose and 0.2% Tween 80) or compound in vehicle (0.5% methylcellulose and 0.2%
49
50 Tween 80) at 10 mg/kg. Each group consisted of 10 mice, with 3 laser burns to each eye yielding
51
52 60 data per group.
53
54
55
56
57
58
59
60

1
2
3 Laser photocoagulation. Mouse pupils were dilated with one drop (volume 40 μ l) of 1%
4 cyclopentolate. Just before anesthesia, pupil dilation was maximized with an additional drop of
5 phenylephrine (usually 10% but occasionally 2.5% depending upon availability). Mice were
6 then anaesthetized with an intraperitoneal (i.p.) injection of a mixture of ketamine and xylazine
7 at dosed up to 100 mg/kg and 10 mg/kg, respectively. Prior to laser pulse application, each eye
8 was anesthetized with topical 0.5% proparacaine. Lubricating eyedrops (Genteals® Novartis) on
9 a glass cover slip was applied to the cornea, and the retina was viewed through a slit lamp
10 microscope. Three laser pulses were applied to the fundus around the optic nerve of each eye,
11 six laser pulses in total for each mouse. The pulses were from a green laser (wavelength = 532
12 nm; Oculight® GLx) and had a duration of 30 milliseconds, a power of 120 milliwatts, and a
13 spot size of 100 microns. A successful laser burn generated a yellow vaporization bubble which
14 correlated with a rupture of Bruch's membrane. If a vaporization bubble did not form, one
15 additional laser pulse would be administered to the same spot. For each eye a maximum of four
16 shots were allowed. An additional fourth shot was required in fewer than 3% of eyes. After the
17 application of laser burns to both eyes, antibiotic ointment (0.5% Erythromycin, Tobramycin or
18 Neomycin ophthalmic ointment depending on availability and cost) was applied to both eyes.

19
20
21
22
23
24
25
26
27
28
29
30
31
32
33
34
35
36
37
38
39
40
41 Harvest and photography of CNV lesions. Unless indicated, studies were completed 7 days
42 after laser photocoagulation. On the final study day, 0.1 ml of a 5 mg/ml solution of FITC
43 concanavalin-A (Vector Laboratories) was injected intravenously (i.v.) to fluorescently label
44 vascular endothelium. Animals were sacrificed 15 - 30 minutes later with inhaled carbon
45 dioxide. Eyes were enucleated and fixed in 4% paraformaldehyde for approximately 60 minutes
46 at room temperature and then transferred to vials of PBS. Posterior eye cups were dissected
47 from the eyes. The RPE-choroidal-sclera complexes were separated from the neural retina and
48
49
50
51
52
53
54
55
56
57
58
59
60

1
2
3 mounted on microscope slides, at which time each eye was given a randomization code to mask
4
5 the examiners. Fluorescent images of each CNV lesion were photographed with an AxioCam
6
7 MR3 camera on an Axio Image M1 microscope (Zeiss). CNV area was quantified using a semi-
8
9 automated analysis program (Axiovision software version 4.5 Zeiss) that outlined the fluorescent
10
11 blood vessels. Image capture, CNV area measurement, and exclusions (see below) were
12
13 performed on masked microscope slides.
14
15

16
17 Measurements of neovascular lesions. Most eyes generated three data points corresponding to
18
19 the area of each of the three laser-induced CNV lesions. A cohort of 10 mice with both eyes
20
21 treated would optimally provide 60 data points. However, a lesion would be necessarily
22
23 excluded for any of the following reasons: 1) there was choroidal hemorrhage encroaching on
24
25 the lesion; 2) the lesion was of irregular shape indicating an asymmetrical laser burn; 3) the
26
27 lesion had fused with another lesion; 4) the lesion had a size indicating it was an outlier lesion,
28
29 defined below; or 5) the lesion was the only lesion in an eye (i.e., if 2 of the 3 lesions in an eye
30
31 were excluded, then all lesions in that eye were excluded).
32
33
34
35

36
37 An outlier lesion fell into one of the following three categories: 1) “too big”: i.e., it was over
38
39 10,000 μ^2 in area and it was more than 5 times larger than the next biggest lesions in the eye (for
40
41 reference, the mean area of CNV in a control group typically ranged from 10,000 to 20,000 μ^2);
42
43 2) “too small”: i.e., it was less than 1/5 the area of the other next smallest lesion in the eye; this
44
45 criterion applied only if at least one lesion in the eye was over 5,000 μ^2 ; 3) “too different”: i.e.,
46
47 after all of the lesions in a specific treatment group were measured, the lesion’s area was 5-fold
48
49 greater than the mean for that group; this criterion applied only for lesions that were $\geq 5,000 \mu^2$.
50
51
52

53
54 Other reasons that lesions were excluded or not measured include: 1) the death of a mouse
55
56 before the end of an experiment; 2) the failure of the i.v. injection of the vascular label; 3) the
57
58
59
60

1
2
3 laser could not be applied due to media opacities (e.g., a pre-existing corneal scar or cataract); in
4
5 this case the fellow eye could still be included; 4) there was damage to the CNV lesion during
6
7 tissue processing (if any part of the CNV was cut or not discernible, it was not included); and 5)
8
9 a CNV lesion could not be located during the imaging of an eyecup.
10
11
12
13
14
15

16 **Rat Laser-Induced Choroidal Neovascularization (CNV) Model.**

17
18 We used male Brown Norway rats that were typically 12 weeks old (range of age 7 – 14 weeks).
19
20 Rats were purchased from Harlan, rats used in a single experiment arrived at our research facility
21
22 in a single shipment and were age-matched. Experimental interventions for a cohort of animals
23
24 were started on the same day. Laser application for an individual experiment was by a single
25
26 scientist. Cages were randomly assigned to treatment groups with rats sharing a cage receiving
27
28 the same treatment. Animal research presented in this paper was approved by the Novartis
29
30 Institutes for Biomedical Research IACUC Committee.
31
32
33
34
35

36 **Laser photocoagulation**

37
38 Rat pupils were dilated with one drop (volume ~ 40 μ l) of 1% cyclopentolate. Just before
39
40 anesthesia, pupil dilation was maximized with an additional drop of phenylephrine (usually 10%
41
42 but occasionally 2.5% depending upon availability). Rats were then anaesthetized with an
43
44 intraperitoneal (i.p.) injection of a mixture of ketamine and xylazine at doses of 40 - 80 mg/kg
45
46 and 5 - 10 mg/kg, respectively. Prior to laser pulse application, each eye was anesthetized with
47
48 topical 0.5% proparacaine. Lubricating eyedrops (Gentel® Alcon Laboratories, Fort Worth,
49
50 TX) on a glass cover slip were applied to the cornea, and the retina was viewed through a slit
51
52 lamp microscope. Each laser pulse was applied approximately 1 mm from the optic nerve; single
53
54 pulses in each of four separate locations were applied to each eye for a total of eight laser
55
56
57
58
59
60

1
2
3 photocoagulation sites for each mouse. The pulses were from a green laser (wavelength = 532
4 nm; Oculight® GLx Mountain View, CA) and had a duration of 30 milliseconds, a power of 190
5 milliwatts, and a spot size of 200 microns. A successful laser pulse generated a yellow
6 vaporization bubble which correlated with a rupture of Bruch's membrane (evaluated
7 histologically in control rats sacrificed 6 hours after lasering; data not shown). In cases when a
8 vaporization bubble did not form (< 1% of laser pulses), one additional laser pulse could be
9 administered to the same spot. For each eye, a maximum of five laser pulses were allowed to
10 generate 4 lesions. After the application of laser burns to both eyes, antibiotic ointment
11 (Tobramycin or Neomycin ophthalmic ointment depending on availability and cost) was applied
12 to both eyes.
13
14
15
16
17
18
19
20
21
22
23
24
25
26
27

28 **Tissue processing, imaging and CNV area quantification**

29
30

31 Analysis of neovascularization was completed on tissues harvested 11, 12 days or 14 days after
32 laser photocoagulation depending on the dosing paradigm of the experiment. For an individual
33 experiment, all rats were euthanized on the same day after laser photocoagulation. On the final
34 study day, 0.2 ml of a 12.5 mg/ml solution of a 2,000 kD FITC dextran, (Sigma) was injected
35 intravenously (i.v.) to fluorescently label vascular endothelium. Animals were euthanized 15 -
36 30 minutes later with inhaled carbon dioxide. Eyes were enucleated and fixed in 4%
37 paraformaldehyde (Vector Laboratories, Burlingame, CA) for approximately 60 minutes at room
38 temperature, and then the fixative was replaced with PBS. Each eye was assigned a randomized
39 number to mask the samples for the remainder of the analysis. Posterior segments were isolated
40 and retinas were removed. The posterior eye cups which included the retinal pigment epithelium
41 (RPE), the choroid, and the sclera, were flat-mounted onto microscope slides after making 3 or 4
42 radial cuts. Fluorescent images of each CNV lesion were photographed with an Axiocam MR3
43
44
45
46
47
48
49
50
51
52
53
54
55
56
57
58
59
60

1
2
3 camera on an Axio Image M1 microscope (Carl Zeiss Microscopy, Thornwood, NY). CNV area
4
5 was quantified using a semi-automated analysis program (Axiovision software version 4.5, Carl
6
7 Zeiss Microscopy) that outlined the fluorescent blood vessels. Image capture, CNV area
8
9 measurement and exclusions (see below) were performed on randomized samples or data by
10
11 scientists masked to the treatment group.
12
13
14

15 16 **Compound administration**

17
18
19 Test articles that were administered via oral gavage, starting approximately 1 hour before
20
21
22 lasering unless described otherwise.
23
24

25 26 **Application of exclusion criteria**

27
28 Each eye typically generates 4 data points corresponding to the area of 4 individual CNV lesions.
29
30 In a typical study, a cohort of 10 rats per group would optimally provide 80 data points.
31
32 However, a lesion would be excluded for any of the following reasons: 1) there was choroidal
33
34 hemorrhage encroaching on the lesion; 2) the lesion was linear instead of circular, a consequence
35
36 of a deflected (“split”) laser impact; 3) the lesion had fused with another lesion; 4) the lesion had
37
38 a size indicating it was an outlier lesion as defined below; or 5) the lesion was the only lesion in
39
40 an eye (i.e., if 3 of the 4 lesions in an eye were excluded, then all lesions in that eye were
41
42 excluded).
43
44
45
46
47
48
49
50
51

52 An outlier lesion fell into one of the following three categories: 1) “too big”: i.e., it was over
53
54 10,000 μ^2 in area and was more than 5 times larger than the next biggest lesion in the eye (for
55
56 reference, the mean area of CNV in a control group typically ranged from 10,000 to 20,000 μ^2);
57
58
59
60

1
2
3 2) “too small”: i.e., it was less than 1/5 the area of the next smallest lesion in the eye; this
4
5 criterion applied only if at least one lesion in the eye was over 5,000 μ^2 ; 3) “too different”: i.e.,
6
7 after all of the lesions in a specific treatment group were measured, the lesion’s area was 5-fold
8
9 greater than the mean for that group; this criterion applied only for lesions that were $\geq 5,000 \mu^2$.
10
11

12
13
14 Other reasons that lesions were excluded or not measured include: 1) the death of a rat before the
15
16 end of an experiment; 2) the failure of the i.v. injection of the vascular label; 3) media opacities
17
18 precluding accurate laser application (e.g., a pre-existing corneal scar or cataract); in this case the
19
20 fellow eye could still be included; 4) damage to the CNV lesion during tissue processing (i.e.,
21
22 poor quality of the tissue during processing so that the lesion could not be fully delineated); 5)
23
24 inability to locate a CNV lesion during the imaging of an eyecup.
25
26
27
28
29
30
31

32 **Ocular PK in Brown Norway Rats Following Administration of a Single Oral Dose.**

33
34
35

36 Three month old Brown Norway rats were administered orally with active agent of Table 5 at
37
38 the dosing concentration and formulation specified. Ocular tissues and plasma were collected
39
40 from 2 rats per active agent at 6, 24, 48, 72, 96, 120 and 144 hrs after dosing. The ocular tissues
41
42 collected were the retina and the posterior eye cup. Each time point had drug levels measured in
43
44 4 individual retinas, 4 individual posterior eye cups and 2 individual plasma samples.
45
46
47

48 Ocular tissues were homogenized and plasma proteins precipitated and drug concentration
49
50 was analyzed by LC-MS/MS. Exposures in the Retina, Posterior Eye Cup (PEC) and plasma for
51
52 the compounds were dose normalized and are listed in Table 5 as area under the curve
53
54 measurements (AUC), C_{max} , and C_{24hrs} .
55
56
57
58
59
60

1
2
3
4
5
6
7
8
9
10
11
12
13
14
15
16
17
18
19
20
21
22
23
24
25
26
27
28
29
30
31
32
33
34
35
36
37
38
39
40
41
42
43
44
45
46
47
48
49
50
51
52
53
54
55
56
57
58
59
60